The spatial ecology of climate influences species distributions: the case of North American amphibians

Gabrielle Lea Rimok

A Thesis
in
The Department of Biology

Presented in Partial Fulfillment of the Requirements
for the Degree of Masters of Science (Biology)
at Concordia University
Montréal, Québec, Canada

November 2021

Concordia University

School of Graduate Studies

This is to certify that the thesis prepared

By: Gabrielle Lea Rimok

Entitled: The spatial ecology of climate influence species distributions: the case of North American amphibians

and submitted in partial fulfillment of the requirements for the degree of

Master of Science (Biology)

Complies with the regulations of the University and meets the accepted standards with respect to originality and quality.

Signed by the final Examining Committee:

Dr. Selvadurai Dayanandan	Chair
Dr. Jean-Philippe Lessard	Examiner
Dr. Carly Ziter	Examiner
Dr. James Grant	External Examiner
Dr. Pedro Peres-Neto	Thesis Supervisor

Approved by:

Dr. Robert Weladji

Graduate Program Director

Dr. Pascale Sicotte

Dean of Faculty

Date: November 15th 2021

ABSTRACT

Title: The spatial ecology of climate influences species distributions: the case of North American amphibians

Author: Gabrielle Lea Rimok

Species distributions are largely determined by three main drivers: abiotic environmental conditions, dispersal, and biotic interactions. Because abiotic environmental conditions determine habitat suitability, they also have direct implications on the capacity of species to disperse and how species interact with one another in space. However, it is specifically the variability in abiotic environmental conditions (i.e., environmental heterogeneity) and how they are spatially structured (i.e., environmental spatial autocorrelation - ESA) that determines whether or not a habitat, or even a landscape, is environmentally suitable for species establishment. Environmental heterogeneity itself is spatially structured; where environmental conditions/features that are closer together in space tend to be more similar than those farther apart. As such, the spatial structure of environmental features (i.e., ESA) mimics dispersal networks because spatial patterns in environmental heterogeneity affect the strategies and energetic costs (and their associated fitness consequences) involved in movement and dispersal among patches. At broad spatial scales, species distributions are shaped by environmental conditions, namely, those of climate. Climatic conditions thus also impose important physiological and life history constraints on species and in accordance with environmental features, are also often heterogeneous and spatially structured. Yet, how they affect and contribute to species distributions remains unknown. Here, we use species distribution models (SDMs) in a novel framework in which we demonstrate for the first time, the influence of climate heterogeneity (within and between patches) and climate spatial structure on species distributions. We evaluated six different SDMs testing both the individual and combined effects of climate variables (i.e., between and within-patch climate heterogeneity and climate spatial structure) on species distributions, using 301 North American amphibian species as a case study. Our results demonstrate that a model using climate spatial structure as a predictor alone explained species distributions better than any other model in the majority of species. Although a model including both climate heterogeneity (within and between-patch) and climate spatial structure as predictors was only the best model for a handful of species, we provide critical evidence that there is added value in considering climate spatial structure when fitting different SDMs for

the same species. Most importantly, we demonstrate that climate spatial structure and heterogeneity are important mechanisms driving species distributions in North America.

ACKNOWLEDGMENTS

I would firstly like to thank both Pedro Henrique Braga (PhD Candidate) and Héctor Vázquez-Rivera (former Post-Doc) from our Community and Quantitative Ecology Lab for the datasets I inherited from them for this study. The resolution of both the IUCN amphibian range maps and WorldClim datasets utilized here are the outcome of extensive manipulation and preparation on their part. I would also like to thank my past and present lab mates for providing some really insightful feedback on my research, helping me resolve data and computation-related roadblocks, and for making me feel welcome and included into such a wonderful lab. It made my graduate experience really memorable, and I am really grateful to all of you.

Above all, I would like to give a big thank you and express my sincerest gratitude to my supervisor and mentor Pedro Peres-Neto. Thank you for always being so comprehensive, understanding, accommodating, empathetic, and forthcoming regarding my health. Thank you for helping me take care of my health so that I could focus on my studies and not only enjoy grad school, but absolutely love my research! I would also like to thank you for giving me the opportunity to study amphibians (which are my life, as you know) and for always sending exciting articles and amphibian-related things my way. Most importantly, I would like to thank you for always answering my millions of questions, for always encouraging me and believing in me, and for sharing your knowledge. Thank you as well for pushing me to solve problems on my own so that I can be a better critical thinker and scientist, and for sharing so much for your time (which is precious and limited) with me. All of these things have made for an amazing graduate experience, and I look forward to continuing our work together over the coming years.

I am eternally grateful to my fiancée Mylène for always believing in me and encouraging me when I was feeling discouraged and stressed out, for always listening to me ramble on about my project, frogs, and reading so many versions of my written work even though this is not remotely related to your field of study. Thank you above all for looking after me when I was sick (which I often was) and when I broke my ankle mere weeks before submitting this thesis. Thank you for helping me be the best version of myself. I am also grateful to my whole family for encouraging and supporting me, and always believing in me and my love of frogs. I am also exceptionally grateful to my late dog Snoopy who I loved so very much and who helped me get through my undergrad and the worst of my Crohn's disease, and to my cat Prima for all the cuddles and love she shares. I would also like to thank my very best of friends Pooja, Catherine, Janina, and Marie-Pascale for being so amazingly supportive, caring, encouraging, and equally geeky about all the things we love! You all make my life so much richer, and I am grateful to have you all in my life.

Lastly, I would like to sincerely thank all those who have given their time to help me during my undergrad and helping me get into grad school. I especially want to thank and all those who have given their time to write letters of recommendation on my behalf, sometimes multiple times: Pedro Peres-Neto, Freida Beauregard, Amanda Babin, Valerie Vien, Martina Strömvik, George McCourt, Raja Sengupta, Jeffrey Cardille, James Fyles, and Norman Lévesque. Thank you all for your support and kind words over the years.

My research would not have been possible without the financial support of the FRQNT (B1X – Bourse de maîtrise), Concordia University (NSER special Entrance Scholarship), the QCBS for the BIO860M intensive course scholarship, and Pedro Peres-Neto for funding an international course on species distribution modelling and funding my studies in the extra semester it took for me to complete my masters degree.

TABLE OF CONTENTS

LIST OF TABLES AND FIGURES ..... **VII**

LIST OF SYMBOLS AND ABBREVIATIONS ..... **IX**

INTRODUCTION **1**

METHODS **8**

RESULTS **16**

DISCUSSION **19**

CONCLUSION **26**

REFERENCES **27**

FIGURES **38**

TABLES **53**

APPENDIX I **54**

APPENDIX II **55**

LIST OF TABLES AND FIGURES

In-text Tables and Figures

Figure 1: Fictional example of the proposed modelling framework for a landscape with 2500 cells (50 x 50 cells).

Figure 2: Illustration of the methodology for preparing the WorldClim climate data to calculate climate heterogeneity between geographic cells (Mean), climate heterogeneity within geographic cells (SD), and local Moran's *I* (LSA).

Figure 3: Ranked model fit (i.e., AIC) across amphibian species for all six species distribution model (SDM) specifications evaluated at different spatial scales for scenarios 1 (i.e., all 301 amphibian species) and 2 (i.e., 127 amphibian species having between 50 and 900 presences).

Figure 4: Proportion (in percentage) of species under scenarios 1 (all 301 species) and 2 (127 species having between 50 and 900 occurrences) associated to mean rankings of model fit (i.e., AIC) for each of the six species distribution model (SDM) specifications at different spatial scales.

Figure 5: Within-model median coefficients rankings across all amphibian species for species distribution model (SDM) specifications of the Mean, SD, and SA of climate at different spatial scales.

Figure 6: Within-model median coefficients rankings across all amphibian species for the species distribution model (SDM) specification with all climate predictors (i.e., Mean + SD + LSA) at different spatial scales.

Figure 7: Group overall within-model median coefficients rankings across all amphibian species for each predictor type (i.e., Mean , SD, and LSA) of the species distribution model specification with all climate predictors at different spatial scales.

Figure 8: Heatmaps of amphibian species clustered by their response to within-model median coefficients rankings for the species distribution model (SDM) specification with all climate predictors (i.e., Mean + SD + LSA) at different spatial scales.

Figure 9: Predictions for the probability of presence in *Anaxyrus cognatus* (Great Plains toad) on continental North America and Hawaii for the predictive species distribution model (SDM) specifications for both the Mean and the all-predictor (i.e., Mean + SD + LSA) climate models at different spatial scales.

Figure 10: Measures of model performance for the predictive species distribution model (SDM) specifications for both the Mean and the all-predictor (i.e., Mean + SD + LSA) climate models at different spatial scales for *Anaxyrus cognatus* (Great Plains toad) on continental North America and Hawaii.

Figure 11: Comparison of the spatial autocorrelation of model residuals between both predictive species distribution model (SDM) specifications at different spatial scales for the case study species *Anaxyrus cognatus* (Great Plains toad).

Table 1: Proportion (%) of amphibian species associated to the average ranking in model fit (i.e., AIC) for all six species distribution model specifications across three different spatial scales and for both scenarios 1 (all 301 amphibian species) and 2 (127 amphibian species having between 50 and 900 occurrences.

Appendix

Table A1: Overall average and median rankings of model fit (based on AIC) for the six species distribution model specifications evaluated across three different spatial scales and for both scenarios 1 (all 301 amphibian species) and 2 (127 amphibian species having between 50 and 900 presences).

LIST OF SYMBOLS AND ABBREVIATIONS

Symbols & abbreviations	Definition
LSA	Local Spatial Autocorrelation
SD	Standard Deviation
Mean	Arithmetic mean
α-diversity	Alpha diversity – species richness of a given patch
β-diversity	Beta diversity – diversity between given patches of a region
γ-diversity	Gamma diversity – total diversity across all patches of a region
SDM	Species Distribution Model
ESA	Environmental Spatial Autocorrelation
LMI	Local Moran's *I*
IUCN	International Union for the Conservation of Nature
TPR	True Positive Rate/Sensitivity
TNR	True Negative Rate/Specificity
Model 1	SDM of the mean of each of the 19 bioclimatic variables (i.e., climate heterogeneity between-geographic supercells)
Model 2	SDM of the standard deviation (SD) of each the 19 bioclimatic variables (i.e., climate heterogeneity within-geographic supercells
Model 3	SDM of the local spatial autocorrelation (LSA) (i.e., Local Moran's *I*) of the mean of each of the 19 bioclimatic variables
Model 4	SDM of the mean and SD of each of the 19 bioclimatic variables
Model 5	SDM of the mean and LSA of the mean of each of the 19 bioclimatic variables
Model 6	SDM of the mean, SD, and LSA of the mean of each of the 19 bioclimatic variables
$P = 301$	Scenario 1: scenario evaluating all presences for all 301 amphibian species
$50 \leq P \leq 900$	Scenario 2: scenario evaluating species having between 50 and 900 presences (127 amphibian species)

INTRODUCTION

The main drivers of species distributions can be broadly attributed to abiotic habitat suitability, dispersal capacity, and biotic interactions (e.g., mutualism, competition, etc.) (Menge and Olson 1990; Guisan and Zimmermann 2000; Guisan and Thuiller 2005; Elith and Leathwick 2009; Ai et al. 2013; Shen et al. 2013; Guisan et al. 2017). Of the three, abiotic habitat suitability (i.e., suitability of abiotic environmental conditions) is likely to be the most relevant in driving species distributions because of its direct implications on dispersal capacity and biotic interactions (Dormann et al. 2007; Ai et al. 2013; Stein et al. 2014; Guisan et al. 2017). To support this, consider the following: for dispersal capacity, if the abiotic environmental conditions between environmentally suitable habitats are extremely unsuitable, then they present a dispersal barrier, thereby limiting the distribution and possible range expansion of the given species (Guisan et al. 2017). For biotic interactions, consider two species with similar habitat and environmental requirements; that is, similar niche breadths (*sensu* Hutchinson 1957). If both species were to occupy a same habitat having optimal (i.e., preferred) abiotic environmental conditions, then they would have to compete with one another for space and access to resources within the given habitat (Stein et al. 2014; Guisan et al. 2017). Ultimately, however, the populations of both species will be limited by the geographic extent of these suitable environmental features (Stein et al. 2014; Guisan et al. 2017). Thus, these two examples provide strong arguments for the role that abiotic environmental conditions play in driving species distributions. More specifically, they emphasize the importance of relationship species have with the features of their abiotic environment.

Species have a strong relationship with their abiotic environment because environmental features themselves have intricate spatial structures that form the complex landscape mosaics we observe in nature (Legendre et al. 2005). As an illustrative example, think of a landscape as a 10,000-piece puzzle; each piece being defined by its unique physical attributes. Individually, each piece contributes valuable information about the image illustrated on the puzzle. Some pieces that are positioned closer together in space may share strong similarities with one another than would be expected by chance (i.e., positive spatial autocorrelation), while other similar pieces may be positioned further apart (i.e., negative spatial autocorrelation) (Legendre 1993; Fortin et al. 2006; 2013). The spatial structure that exists among pieces – a mosaic of different colors, shapes, and patterns – is what contributes to the complex image forming the puzzle (Dufour et al. 2006).

Likewise, patches (i.e., habitats delimited by a set environmental conditions/features in a given geographic space) within landscapes contain environmental features that may or may not be shared by nearby patches, depending on how they are oriented, configured, and distributed in space and time (note here that only space is considered for this study) (Ricklefs 2004; Esparza-Orozco 2020). This complex and systematic (non-random) variation is termed spatial autocorrelation (SA) and is described as both linear and non-linear functions of the joint variation between environment and spatial positioning of patches within a landscape (Dray et al. 2006, Griffith and Peres-Neto 2010). The variation in how environmental features differ from one another is known as environmental heterogeneity (Shen et al. 2013; Donelle 2018).

Taken together, both the heterogeneity and spatial structure of environmental features/conditions are expected to affect species distributions and their relationship with the abiotic environment (Palmer and Dixon 1990; Peres-Neto et al. 2012; Ai et al. 2013; Shen et al. 2013; Stein et al. 2014; Basile et al. 2016; Monteiro et al. 2017; Araújo et al. 2018; Leibold and Chase 2018). Empirical and theoretical work on how environmental heterogeneity underlies species and community dynamics emphasize, almost without exception, how much variation exists among patches (i.e., magnitude of variation; but see Büchi et al. 2009; Shen et al. 2013; Stein et al. 2014; Basile 2016; Monteiro et al. 2017; Donelle 2018). Nonetheless, environmental heterogeneity is spatially structured (autocorrelated) as the norm rather than at random (Donelle 2018). Two landscapes can be similar in their environmental heterogeneity (i.e., variance among patches) but differ in how their environmental features (resources and non-resources) are structured in space (Peres-Neto et al. 2012). Spatial autocorrelation corresponds to the size of distributions of suitable and unsuitable patches and how smooth their transitions (differences) are as a function of distance among patches in a landscape. Under weak spatial autocorrelation, patches vary more (probabilistically) in their environmental features in relation to one another (i.e., smaller clusters of patches having similar environmental conditions); whereas strong autocorrelation represents large clusters of patches composed of similar environmental conditions. The steepness of environmental variation among clusters of patches can also be described by a statistical representation of spatial autocorrelation. In many cases, the spatial structure of environmental features mimics dispersal networks because spatial patterns of environmental heterogeneity affect

the strategies and energetic costs (and associated fitness consequences) involved in movement and dispersal among patches (Peres-Neto et al. 2012; Shen et al. 2013).

It is expected then that species' environmental tolerances and affinities have been shaped over ecological and even evolutionary time as functions of the spatial structure of the environment (i.e., Environmental Spatial Autocorrelation – ESA) (Kassen 2002; Vellend 2010; Katayama et al. 2014; Donelle 2018). For example, resource generalists may be less sensitive and, consequently, adapted to environmentally heterogeneous landscapes regardless of landscape ESA, whereas resource specialists are expected to be more sensitive to the size of environmental clusters in a landscape (Büchi and Vuilleumier 2014). This is because of energetic costs involved in dispersal. Because ESAs represent how abrupt, sharp, or predictable changes in environmental conditions can be in space, movement and dispersal costs are expected to be higher in landscapes having weak ESAs (i.e., more abrupt transitions among patches). As a result, because generalists have wide niche-breaths, their energetic costs are expected to be lower while dispersing through landscapes with weak ESA (Büchi and Vuilleumier 2014; Donelle 2018). Generalists also benefit from the availability of multiple habitat types and reduced competition with specialists (Kassen 2002; Büchi and Vuilleumier 2014; Vellend 2010; Donelle 2018). Due to their narrow niche-breadths, specialists should perform better where ESA is stronger because they contain greater clusters of similar patches (Büchi and Vuilleumier 2014; Donelle 2018).

At broad spatial scales, species distributions are largely determined by abiotic environmental conditions, notably, those of climate (Guisan et al. 2017; Tordoni et al. 2020). Likewise to environmental conditions, climatic features are also often spatially structured and fragmented (Fujiwara and Takada 2017; D'Amen et al. 2017; Fournier et al. 2020). Climate conditions impose important physiological and life history constraints on species. As such, we expect that the spatial configuration and variability of climatic conditions should also underly species distributions and the structure of their communities. Indeed, a recent study exploring how the frequency of climatic types (i.e., the commonality or rarity of climatic conditions) affects biodiversity corroborates this hypothesis (Fournier et al. 2020). They demonstrated that patches containing rare climates (which were shown to be more spatially dispersed), yield a larger proportion of generalists in relation to specialist species (Fournier et al. 2020). Adapting to rare resources and environmental features is evolutionarily costly (Kassen 2002). Species with wide

niche-breadths (generalists) should then tend to be favored in rare climates in relation to specialist species that should outcompete generalists in more frequent climates (Fournier et al. 2020). Taken together, ESA should be an important factor because of the way it can constrain or facilitate species responses to environmental heterogeneity and, moreover, mediate the co-existence of species that vary in niche requirements and breadths (i.e., generalists versus specialists) and dispersal capacities.

As such, species distributions should then vary as a function of niche breadth, dispersal capacity, and the strength of ESA of a given landscape. In landscapes with weak ESA, we might expect that the distributions of species overlap one another strongly and be located in and around clusters of suitable climatic/environmental conditions, where there is a larger proportion species distributions for species with strong dispersal capacities and wide niche-breadth than species with weak dispersal capacities and narrow niche-breaths (Donelle 2018; Fournier et al. 2020). Distributions for strong dispersers and species with wide niche-breadths may then generally be larger than the distributions of their counterparts and may be generally broader in area than the geographic extent of climatic/environmental clusters with suitable conditions. Conversely, we might expect that the distributions of species in landscapes with strong ESA only somewhat overlap one another and tend to closely follow the geographic extent of clusters of suitable climatic/environmental conditions. For poor dispersers and species with narrow niche-breadths, their distributions may overlap one another to some degree, but will mostly be partitioned within the geographic extent of clusters with suitable climatic/environmental conditions, facilitating coexistence (Büchi and Vuilleumier 2014; Donelle 2018; Leibold and Chase 2018). In landscapes with strong ESA, these species are also likely to occur in a greater proportion relative to their non-dispersal limited and wide-niche breadth counterparts because they are superior competitors (Donelle 2018). However, species with wide niche-breadth and strong dispersal capacities will likely have distributions that frequently overlap those of their dispersal-limited and narrow niche-breadth counterparts in both landscapes with strong and weak ESA. This is because they are, in general, more resistant to unsuitable climatic/environmental conditions (Büchi and Vuilleumier 2014). Their resistance to these unsuitable conditions allows their distributions to be much broader, encompassing a greater geographic area, thereby allowing them to seek and establish themselves at vacant sites more readily (Büchi and Vuilleumier 2014; Donelle 2018).

Because environmental/climatic heterogeneity and spatial structure have direct implications on dispersal and niche-breadth, as detailed above, they consequently also interact with processes of community assembly (e.g., species sorting, dispersal, coexistence) (Cornell and Lawton 1992; Chesson 2000; Ricklefs 2004; Dufour et al. 2006; Peres-Neto et al. 2012; Katayama et al. 2014; Stein et al. 2014; Araújo et al. 2018; Esparza-Orozco et al. 2020). For instance, species sorting posits that at low dispersal rates, species are sorted in the landscape according to their habit preferences and availability of resources (Leibold et al. 2004; Vellend 2010; Esparza-Orozco 2020). Thus, for a landscape to support species with low dispersal capacities, it should have strong ESA because connectivity between suitable sites is facilitated, which consequently decreases energetic costs related to dispersal (Donelle 2018). Most importantly, a landscape with strong ESA would facilitate species coexistence because for species to persist, they must partition their resources (Chesson 2000; Mouquet and Loreau 2002; Vellend 2010; Logue et al. 2011; Donelle 2018; Ben-Hur and Kadmon 2020). As such, the interactions between dispersal, species interactions, differences in species niches (position and tolerance), and environmental heterogeneity are complex and generate much of the contingency observed in ecological populations and communities (Catford et al. 2021; Leibold et al. 2021).

The goal of this paper is to test the hypothesis that the spatial structure of climate features is relevant in explaining species distributions. We use species distributions models (SDMs) to estimate the contributions of climate heterogeneity among patches, climate variation within patches, and the spatial structure of climate (note here that 'patches' hereafter refers to georeferenced cells containing species occurrence and climate data). Species distribution models, otherwise known as Climate Envelope Models among other names (Elith and Leathwick 2009; Jarvie and Svenning 2018), quantitatively relate empirical observations of species occurrences to the environmental characteristics that define their occupied niche (Guisan and Thuiller 2005; Mielke et al. 2020). Fundamentally, SDMs infer that the distribution and size of terrestrial species' ranges are governed by the distribution of climate patches within landscapes (Pearson and Dawson 2003; Elith and Leathwick 2009; Garcia et al. 2014; Guan et al. 2020). Spatial autocorrelation and consequently, ESA, have been historically treated as a statistical nuisance in SDMs and models of biodiversity across space (e.g., variation in beta-diversity in relation to environmental features across space); an effect needing to be controlled and accounted for in these models (Legendre 1993;

Perry et al. 2002; Griffith and Peres-Neto 2006; Dormann et al. 2007; Record et al. 2013). As such, ESA is then treated as a confounding variable, resulting from the correlation between spatial and environmental parameters, and when present in model residuals, affects tests of significance and uncertainty in model parameter estimates (Legendre 1993; Perry et al. 2002; Griffith and Peres-Neto 2006; Peres-Neto and Legendre 2010; Record et al. 2013). Failure to account for spatial autocorrelation in model parameters (e.g., climate variables) can lead to dubious predictions and incorrect conclusions, resulting in a misleading narrative about the preferred niche characteristics of a given species (Mielke et al. 2020). As such, the spatial structure of environmental features in ecological models is usually discarded as a nuisance and only the sources of environmental heterogeneity that are not spatially structured are interpreted. Another goal of controlling for autocorrelation is to improve model transferability to other landscapes that may present very different spatial autocorrelation structures in their environmental (climatic) features (Araújo et al. 2005).

Beyond the statistical challenges generated by spatial autocorrelation, as discussed above, there is strong indirect evidence that the spatial structure of environmental features should be an important factor in dictating species distributions and the composition of communities. Indeed, the shared predicted variation between spatial predictors and environmental features in the variation partitioning of species distributions and beta-diversity models is often strong (Legendre 1993; Cottenie 2005; Diniz-Filho and Bini 2005; Beisner et al. 2006; Peres-Neto et al. 2006; Costa et al. 2007; Huang et al. 2011; Peres-Neto et al. 2012; Rojas-Ahumada et al. 2012; Provete et al. 2014; Donelle 2018; Hsiung et al. 2017; Kumar et al. 2019). There are many ways to build these spatial predictors (e.g., Dray et al. 2006; Griffith and Peres-Neto 2006; Dormann et al. 2007). They capture what we refer to as latent spatial structures, by building spatial functions (e.g., Fourier spectral decomposition, spatial polynomials, splines spatial covariance matrices, spatial eigenvectors) that are included in the model to capture spatial autocorrelation in species distributions (e.g., Cottenie 2005; Griffith and Peres-Neto 2006) or attenuate residual variation while fitting SDMs (e.g., Dormann et al. 2007). In this sense, currently used spatial functions represent unknown sources (latents) of variation in SDMs and community models because they do not represent the spatial variation of environmental predictors (climatic features), but rather, the variation in the response (e.g., species distribution, beta-diversity). These latent spatial functions represent global spatial

autocorrelation (average spatial structure for a given environmental feature) and, as such, cannot describe the location of clusters of similar and dissimilar patches. Moreover, many of these global function models only represent positive autocorrelation as the source generating bias in statistical models. However, negative autocorrelation can be also important in driving species and community dynamics (Biswas et al. 2017). Finally, global spatial autocorrelation functions mix both positive and negative autocorrelation patterns, which can lead to an absence of spatial autocorrelation, given they globally negate each other statistically (Dray 2011).

Here, instead, we propose using Local Indicators of Spatial Association (LISA) to quantify the joint covariance (i.e., similarity) between neighbouring patches and their climate features (Anselin 1995). We use the local Moran's I (LMI) coefficient of spatial correlation to describe the spatial patterning of climatic variables and use them as predictors in ecological models. Popular applications of LMI include identifying spatial clusters, patterns, and hotspots of chemical elements in urban soils and forests (see Zhang et al. 2008; Fu et al. 2014; Yuan et al. 2018; Tepanosyan et al. 2019) and examining how model residuals are spatially clustered and distributed in ecological models (see Zhang et al. 2005; Osborne et al. 2007; Smulders et al. 2010). Figure 1 provides an overview of the proposed framework for a fictional simulated species that prefers warm temperatures but is only present in patches within large clusters of warm temperatures. In addition to climate heterogeneity (changes across patches) and local SA, we also considered climate heterogeneity within patches, quantified via the standard deviation of climate predictors within geographic cells (see Choi et al. 2014; Singh and Goyal 2016).

In addition to the proposed new framework for SDMs that considers additional predictors (i.e., beyond the commonly used climate heterogeneity among patches) based on local spatial autocorrelation of climate features and climate heterogeneity within patches, we provide an empirical test of its performance using amphibians as a case study. Of all vertebrate classes, amphibians are the most threatened by extinction, thereby highlighting their importance in ecological research (Catenazzi 2015). Their semi-aquatic and semi-terrestrial life history additionally renders them as unique and relevant bioindicators of environmental health and quality (Bishop et al. 2012). Amphibians are also highly sensitive to and strongly affected by climatic conditions, particularly precipitation and temperature (Corn 2005; Lannoo 2005; Rodríguez et al. 2005; Qian et al. 2007; Diniz-Filho et al. 2008; Brodman 2009; Hof 2010; Qian 2010; Huang et al.

2011; Silva et al. 2011; Ortiz-Yusty et al. 2013; Cohen et al. 2016; Araújo et al. 2018). Variation (i.e., spatial structure and heterogeneity) in climatic conditions can have important biological consequences on their fitness, dispersal, persistence, adaptability, richness, and diversity, making them a well-suited organismal group for this study (Blaustein et al. 1994; Alford and Richards 1999; Wind 1999; Boone et al. 2003; Lannoo 2005; Rodríguez et al. 2005; Smith and Green 2005; Brodman 2009; Miller et al. 2018; Joly 2019). Finally, amphibians are the vertebrate class with the highest proportion of data-deficient species (Howard and Bickford 2014). This makes them an especially pertinent taxonomic class on which to test our new modelling framework because we can expect similar if not stronger results in other vertebrate classes not affected by a lack of available data (such as birds and mammals) (Titley et al. 2017). Accordingly, we thus predict that the inclusion of both within-patch climate heterogeneity and climate spatial structure as explanatory variables in SDMs (in addition to the standard use of climate heterogeneity among patches) will strongly contribute to explaining the distributions of amphibian species.

METHODS

Amphibian data

We obtained occurrence data for amphibians from the International Union for the Conservation of Nature (IUCN) in the form of global digital distribution (range) maps (IUCN 2018). IUCN range maps are the sole global-scale range maps available for amphibians, making them the leading authority as a comprehensive broad-scale taxonomic and geographic database for this vertebrate class (Di Marco et al. 2017). These range maps are commonly used in global and regional scale macroecological analyses in the biogeography, ecology, evolution, and conservation planning and management of amphibians (Ficetola et al. 2014; Di Marco et al. 2017).

Climate data

We obtained high spatial resolution (i.e., 5 x 5 km) gridded climate data in the form of 19 bioclimatic variables (referred to here on as 'bioclim data') from WorldClim (see **APPENDIX I** for more details). These 19 bioclim variables encompass annual trends, seasonality, and limiting or extreme climatic factors, in which 11 relate to temperature, and the remaining 8, to precipitation

(Fick and Hijmans 2017). These data represent the average climatic conditions from the years 1970 to 2000 and are the most used in SDMs (Fick and Hijmans 2017).

Data preparation

Both the IUCN range maps and WorldClim datasets were manipulated to have the same spatial resolution of 50 x 50 km with matching origins, with the WorldClim data containing 100 equally-spaced geo-referenced data points within each 50 x 50 km cell. Using the *sp* (Pebesma and Bivand 2005) and *sf* R packages (Pebesma 2018) to spatially align the datasets to North America, both global-scaled datasets were reprojected from the Pseudo-Mercator projection (EPSG: 3857) to the Azimuthal Equidistant projection, centered at the centroid of the continent. Only data lying within the boundary of continental North America and Hawaii were retained. Initially, the global IUCN range maps used here contained data for 6491 amphibian species, and after reducing their global extent to that of continental North America, 301 species remained. Next, the bioclim data were further reduced to match the extent of the amphibian data, which excludes the arctic and parts of northern Canada and Alaska. To match the resolution of the bioclim data to that of the IUCN, the mean ($\bar{\boldsymbol{X}}$) was calculated across all 100 5 x 5 km cells encompassed within each 50 x 50 km "supercell" (Fig. 2) out of 7035 supercells0

. This variation across supercells in their mean values $\bar{\boldsymbol{X}}$ represent climate heterogeneity across geographic supercells and is the most used in SDMs. Climate heterogeneity within geographic supercells was based on the standard deviation $\boldsymbol{s}$ (hereafter referred as SD) across the 100 5 x 5 km cells for each supercell (Fig. 2). These manipulations resulted in a single geo-referenced value for the Mean $\bar{X}$ and SD for each of the 19 bioclim variables lying within each 50 x 50 km geographic supercell.

We used Local Moran's *I* to estimate the local spatial autocorrelation (LSA) for each climate (bioclim) variable for each geographic supercell *i* as:

$$I_i(LSA) = \frac{X_i - \bar{X}}{s_i^2} \sum_{j=1, j \neq i}^{n} \omega_{ij}\left(X_j - \bar{X}\right)$$

where X_i is the value of a given mean climate variable within the focal geographic supercell *i* (i.e., mean across all 100 5 x 5 km cells within a 50 x 50 km supercell), $\bar{X}$ represents the average value

for the climate variable of interest across all geographic cells (i.e., North America), s_i^2 is the variance of climate values of all geographic cells excluding the focal cell *i* (see below), and X_j represents the value of the variable at all other cells, excluding the focal site X_i (i.e., where $j \neq i$). ω_{ij} represents the weighted inverse of the pairwise distances $(1/d_{ij})$ between sites i and j. One can certainly consider other functions of the geographic distance (e.g., negative exponential) that better represent how species perceive the size of grains of their environments. Future implementations could consider other functions and assess which ones best fit with the species of interest. For completion, s_i^2 is calculated as:

$$s_i^2 = \frac{\sum_{j=1, j\neq i}^{n} \left(X_j - \bar{X}\right)^2}{n-1}$$

where *n* is the total number of geographic cells (here North America). Thus, I_i defines the Local Moran's *I* (LMI) for each given georeferenced cell containing bioclim data for a given climate variable (Anselin 1995; Zhang et al. 2008) (see Fig. 2). Because we considered 19 climate variables, we have a local I_i for each of the 7035 supercells for each climate variable. A high positive LMI value indicates that a given supercell ($\boldsymbol{X_i}$) has a high number of surrounding supercells (spatial cluster) with similar values. Conversely, a high, but negative LMI value indicates that the given site under observation ($\boldsymbol{X_i}$) is clearly different in its value in relation to the values of neighbouring sites ($\boldsymbol{X_j}$) (Anselin 1995; Zhang et al. 2008; Yuan et al. 2018). These can also form spatial clusters, but they are isolated from one another. These clusters can describe high values in low value neighbourhoods (hotspots) or low values in high value neighbourhoods (cool spots) (Anselin 1995; Zhang et al. 2008; Yuan et al. 2018).

The climate data for species distribution modelling resulted in a total of 7035 50 x 50 km supercells containing the mean (i.e., mean (Mean) values across all 100 5 x 5 km cells within each 7035 supercell of 50 x 50 km, representing environmental heterogeneity between supercells), the standard deviation (standard deviation (SD) for the 100 5 x 5 km cells within each 7035 supercell of 50 x 50 km, representing environmental heterogeneity within supercells) and the Local Moran's *I* (LSA) for each geographic supercell. Again, the species data were occurrences for 301 amphibian species across all 7035 geographic supercells.

Generation of background data for SDMs

The amphibian IUCN range maps are presence-only data. To be used in many of the statistical procedures to fit SDMs, they must also contain 'absences' (often referred as to pseudo-absences or background absences in the SDM literature). Background absences represent the climatic conditions at sites (here supercells) where species have not been recorded as present (Peterson et al. 2011; Araújo et al. 2019; Warren et al. 2021). Background data were produced for each species separately within three circular buffers representing 40%, 60%, and 80% of the maximum geographic distance between all pairwise cells (i.e., supercells) where that species occurs. These pairwise distances were calculated using the Great Circle distance (a geodesic distance metric) on unprojected data using the 1983 North American Datum (NAD83, EPSG: 4269), a geographic coordinate reference system. Calculating pairwise distances in space using projected data uses Euclidean distance, which assumes that the surface is planar. Taking the Euclidean distance over a geodesic surface projected onto a planar surface would cause distortions in these calculated distances (see Flater 2010).

A single background point was then generated for each occurrence of each species, and this process was randomly generated 100 times, resulting in 100 unique possible backgrounds per occurrence, for each species, across 3 buffers. The climate information ($\bar{X}$, SD and LSA) for where the species was present and for each of the background supercells (absences) were collated together and used to fit an SDM (see next section). As such, 300 models (100 background data and 3 buffers) were fit for each species. When a given species had less than the minimum of 50 presences, we resampled additional presences from existing ones so that each species had at least 100 observations (presences plus background absences). For example, if a species had 35 presences, then we would sample 65 background points so that combined the species data had 100 observations (supercells). This was done to avoid model saturation (i.e., few observations compared to the number of predictors) when the number of present cells was too small in relation to the number of predictors. Note, that if we consider all climate variables, we obtain 19 x 3 = 57 predictors (i.e., 19 climate variables times three types of predictors: Mean, SD, and LSA). Here, we used logistic regression to fit SDMs (see next section) which can handle well 57 predictors for 100 observations or more. Depending on the perimeter of a given buffer, in some cases we had no empty cells available from which to sample background points for a particular presence. In this

case, these presences were recorded as such and other presences with potential background points outside of the original buffer were used to account for the difference.

Species Distribution Models

Species distribution models were estimated using a Bayesian logistic regression model (model implemented after Gelman and Hill 2007) assuming a normal distribution of residuals (i.e., normal priors) and a prior mean for the coefficients equal to zero. We used a Bayesian approach for pragmatic reasons such as avoiding convergence issues that often occur with standard logistic regression applied to modelling species distributions. In addition, the standard maximum likelihood approach tends to overestimate the regression coefficients when the number of cells occupied by a species is small in relation to the number of background points (Hefley and Hooten 2015). The model was fit using the *arm* package (version 1.11.2; Gelman and Su 2016) in the R programming environment (version 4.1.1) (R Core Team 2021). Six models with different combinations of the three classes of predictor variables were estimated for each of the 301 species and are represented as presence/background (P/B) ~ : (1) all mean $\bar{X}$ bioclim variables (climate heterogeneity across geographic supercells), (2) standard deviation $\boldsymbol{s}$ (SD) of all bioclim variables (i.e., climate heterogeneity within geographic supercells, i.e., local heterogeneity), (3) Local Moran's I for all the mean bioclim variables (i.e., local spatial autocorrelation (LSA)), (4) the mean $\bar{X}$ and standard deviation (SD) of all bioclim variables (i.e., climate + climate heterogeneity within cells), (5) the mean $\bar{X}$ and local spatial autocorrelation (LSA) of all bioclim variables (i.e., climate + local climate spatial structure), and (6) the mean $\bar{X}$, standard deviation (SD) and local spatial autocorrelation (LSA) of all bioclim variables (i.e., climate + climate heterogeneity within cells + climate local spatial structure). Prior to their inclusion in each of the models, all climate variables were standardized to a mean of 0 and unit variance.

As a case study, we contrasted in greater detail two SDM specifications for an amphibian species (i.e., the Great Plains toad, *Anaxyrus cognatus*) that had a large distribution (i.e., 1107 occurrences), but not extensive enough for its realized niche to be represented by its range: 1) a predictive model using only the mean climate variables; and 2) a predictive model using all variables (i.e., climate, climate heterogeneity, and climate spatial structure).

Model comparisons

We compared the fitted models using the Akaike information criterion (AIC) (Akaike 1974). Note again that 300 models (100 background data and 3 buffers) were fit for each species. Because AIC can only be contrasted among models sharing the same response variable (i.e., using the exact same presences plus background absences), we compared models using ranked AICs as follows. For each unique combination of presence and background data, we ranked the AICs for the six SDM specifications (i.e., resulting from the combination of the three classes of predictors; see above). The models with best fit (lowest AIC) received the highest rank (=1) and the model with the lowest performance received the lowest rank (= 6). We then took the mean of ranks across unique combinations of presence and background data for each buffer for each species. Because climatic suitability and preference varies greatly among amphibian species, their response to climate, climate heterogeneity, and climate spatial structure also vary. As such, we then calculated the proportion (in percentage) of species associated to each of the six ranks for each SDM specification. Two scenarios were considered to represent the results: scenario 1) all 301 species (P = 301); and scenario 2) 127 species having 50 or more presences and 900 or less presences ($50 \leq P \leq 900$). Scenario 2 was created to evaluate the results of the SDMs when filtering for species with too few presences (≤ 50) and a disproportionately large number of presences (≥ 900). Both scenarios were evaluated for each of the three buffers. Because we used species range maps (IUCN based), the number of presences represents the size of species ranges. Comparing model performance across buffers and species range sizes provides a better exploration of model consistency for the six SDM specifications.

It is also costumery in SDMs to use performance metrics based on classification errors (e.g., AUC, i.e., area under the curve, ROC, i.e., receiver operating characteristic curve, number of true positives, true negatives, false positives, and false negatives). Although these metrices can be robust while estimating the discrimination power of one model (i.e., discriminating between presences and absences; but see Hand and Anagnostopoulos 2013), they are not sensitive when comparing across two nested models (i.e., modelling the same response variable). For the extended case study based on *Anaxyrus cognatus*, we estimated different performance metrics including the true positive rate (i.e., model sensitivity or TPR – the number of cells where species is predicted as present and is present), true negative rate (i.e., model specificity or TNR – the number of cells where species is predicted as absent and is absent) and balanced accuracy (i.e., (TPR + TNR)/2).

To estimate these performance metrics, predicted probability values need to be transformed into predicted presences and absences. This is done by applying a threshold probability value in which any predicted probability above the threshold is transformed into a presence and any predicted probability below the threshold is transformed into an absence. Note, however, that the number of occupied geographic cells over the total number of cells dictates the probability in which an uninformative model (i.e., none of the predictors are informative while predicting the species) can predict a species (Olden et al. 2002). Because models are composed of a mix of informative and uninformative predictors, individual threshold values need to be determined for any given model (Nenzén and Araújo 2011). Here, we used a repeated cross validation routine to estimate the probability threshold that optimized the ROC of a particular model (i.e., maximizing TPR while minimizing False Positive Rate, i.e., – the number of cells where a species is predicted as present is actually absent). Other performance metrics led to similar thresholds for our case study species. We resampled 50% of the data (i.e., presences and background data) to fit the model (calibration phase) and the remaining 50% for predicting the probability of presence in each supercell (validation phase). The data were resampled randomly in such a way that the proportion of presences and absences were similar between the training and validation sets. We repeated the cross validation 500 times, producing 500 sets of predicted probability values of presence. The same background data were used in the repeated cross-validation; other background data led to very similar results. We then calculated the median predicted probability value across the 500 sets for each supercell. Based on these median values, we then calculated the ROC for each probability threshold varying from 0.001 to 1.000 (at 0.001 steps, i.e., 1000 thresholds). The threshold that maximized ROC was used to transform all the predicted probability values into either presence or absence. For each of the 500 models based on this threshold, we calculated the true positive rate, true negative rate, and the balanced accuracy. We have also estimated the threshold for each validation set separately instead of using the median across sets but results were nearly identical. For this extended case study (of the species *Anaxyrus cognatus*), we have also compared the levels of spatial autocorrelation in model residuals between the two model specifications used (i.e., predictive model using only the mean climate predictors (heterogeneity across supercells) *versus* a predictive model using all classes of predictors (between-patch climate heterogeneity, within-patch climate heterogeneity, and climate spatial structure). Describing spatial patterns in residual autocorrelation using a correlogram based on global Moran's *I* (across different spatial scales) is a

common procedure in SDM-based studies, and it allows for describing how and at which geographic scales different models contrast in their model performance.

Within-model coefficient comparisons

Model coefficients were also evaluated to explore the variation in predictor relevance across different SDM specifications (i.e., different combinations of the three classes of predictor variables as explained early). Similarly to the ranking process used on model AICs, the absolute values of coefficients were ranked within-model and the median across the 100 background data for each species and spatial buffer was used to evaluate the distribution of coefficients across all species at once. Only models 1 (climate heterogeneity across geographic supercells), 2 (climate heterogeneity within geographic supercells), 3 (local spatial autocorrelation), and 6 (all three classes of predictors) were considered for this analysis. Given models 1, 2, and 3 have 19 coefficients each, the largest coefficient in each model was assigned a rank of 1 (i.e., highest rank) and the smallest coefficient was assigned a rank of 19 (i.e., lowest rank). For model 6 having 57 coefficients, the largest coefficient was assigned a rank of 1 and the smallest coefficient was assigned a rank of 57. Note again that coefficients were ranked based on their absolute values. Median values of ranks within model types across all their 100-background data (for each species and spatial buffer size) were used to estimate overall importance for each predictor. Model intercepts for all four models were excluded from the results. To explore species responses to predictors, we employed a hierarchical cluster analysis to group species based on the similarities of their responses to the predictors used in the last SDM specification (i.e., model with all climate predictors (Mean + SD + LSA)). Predictors were then ordered according to their importance (i.e., median values of ranks across the 100-background data), measured by their coefficient medians across species using a heatmap. We have also calculated ranks for negative and positive coefficients separately. The results for the absolute and signed rankings were very similar and we opted for the latter as they were easier to represent in plots that accentuated and distinguished the importance of coefficients. The hierarchical cluster analysis was run using *hclust* from the *stats* R package (R Core Team 2021; version 4.1.1). Figures and plots were created and represented using the *ggplot2* (Wickham 2016; version 3.3.5) and *lattice* (Sarkar 2008; version 0.20.44) R packages.

RESULTS

Overall model comparisons

The SDM using only local spatial autocorrelation predictors outperformed, on average, the 5 other model specifications regardless of the spatial buffer used to fit them (Fig. 3). SDMs based on mean climate variables (i.e., heterogeneity among geographic supercells) ranked second overall in their performance and SDMs containing only the standard deviation of climate (i.e., heterogeneity within geographic supercells) ranked last. Figure 3 provides more detailed information on how the six model specifications contrasted against one another. The SDM based on spatial autocorrelation ranked as the best model (lowest AIC) in 30.56%, 33.89% and 38.54% all species (i.e., scenario 1) across all spatial buffers (40%, 60% and 80%, respectively; Fig. 4; Table 1). These results were consistent regardless of the species range sizes (Table 1). The model considering only the mean climate (mean values between supercells) consistently ranked second place as the model cumulatively ranking first, second, and third best-fitted model in (minimum) 56.7% to (maximum) 78.7% of species (Fig.4; Table 1), across all spatial scales (i.e., buffers). It is interesting to note that the SDM considering all predictors had the worst performance, on average, when considering all species (Fig. 3; Fig. 4; Table 1; Table A1 in APPENDIX II), but not for species with intermediate ranges, where SDMs considering only climate heterogeneity within sites (i.e., cells) (SD) ranked as the worst model (Table 1).

Within-model coefficient comparisons

Here, we contrasted how predictors ranked within SDMs for four of the SDM specifications that were the most important in contrasting their performance. Figure 5 presents the rank variation across SDMs and species for the models considering only predictors characterizing heterogeneity among geographic supercells, heterogeneity within geographic supercells, or local spatial autocorrelation, whereas Figure 6 presents rank variation in coefficients across species for the model considering all three of these classes of predictors. With increasing buffer size, the coefficients ranking highest and lowest in their medians tended to remain constant (Fig. 5; Fig. 6). The order between the first and last ranked predictors did tend to vary with increasing buffer sizes for each model. For all models, the 60% and 80% buffers varied the least in their order of predictors than under 40% buffer (Fig. 5). Across SDM specifications, however, the bioclimatic predictors

(e.g. BIO1, BIO2, BIO3, etc. (see APPENDIX I)) ranking first through last differed across models. If climate heterogeneity within geographic supercells (SD of climate) and local spatial autocorrelation of the mean climatic variables across geographic supercells (LSA of climate) had no influence on the response of species distributions in North America, then the rank and order of each predictor would, on average, remain the same across all models and species. For model 1, the highest and lowest ranked predictors (Mean 13 and Mean 12, respectively; Fig. 5A) across buffers in increasing order of size were different than those of model 2 (SD 14 and SD 5, respectively; Fig. 5B), model 3 (LSA 7 and LSA 15/13/15, respectively; Fig. 5C), and model 6 (mean: mean 14 and mean 8; SD: SD 11/18/7 and SD 5; LSA: LSA 14/7/7 and LSA 15/18/13, respectively; Fig. 6).

A heatmap displaying the average of ranked coefficients for the model with all predictors further demonstrates that predictors from all three classes of predictors can be relevant in predicting species distributions (Fig. 8). This model's (i.e., model 6) heatmap predictors are not grouped by predictor type but are instead ordered by the importance of each predictor to the overall model across species (Fig. 8). It is interesting to note that the first and last third of predictors (respectively ranking as high and low) appear to have proportionally larger species clusters than the mid-ranked predictors, across all buffers (Fig. 8). This indicates that the most relevant and most irrelevant predictors are shared among many different groups of species whereas there is a lot of variation in species responses regarding coefficients with intermediate predictive power (Fig. 8).

Case study – predictive performance and mapping

Predictions of the probability of presence for the Great Plains toad (*A. cognatus*) varied quite drastically between the mean model (model 1) and the all-variable model (model 6), and across each buffer (Fig. 9). As the buffer size increased for both predictive models, the uncertainty in the predictions of the probability of presence and absence decreased, as illustrated by the decreasing radius of yellow (signifying probability of presence values around 0.4 - 0.6) in the prediction maps (Fig. 9). It is evident that model 6 is the best predictive model for the probability of presence in this species due to the overall higher certainty in its values for predicted presences and absences (Fig. 9). Compared to the predictions of model 1 (climate heterogeneity among supercells), model 6 (with all predictors) had a much narrower halo of probability values that indicate neither the presence nor absence of the species (i.e., the uncertainty prediction zone displayed by the range of colors from light blue to orange; Fig. 9), and this halo shrinks in size as

buffer size increases. As buffer size increases for model 1 (climate heterogeneity among supercells), the extreme north-west predictions in the probability of presence of this species in North America begin disappearing (Fig. 9). This signal is further amplified by model 6 (i.e., with all predictors) where these predictions are simply non-existent. Conversely, model 6 predicts with mid-high certainty that *A. cognatus* is likely to be present in Hawaii and the intersection between the north-western most corner of British Columbia and the south-western most corner of Alaska, whereas these predictions are absent from model 1 (Fig. 9).

Metrics (i.e., balanced accuracy, True Positive Rate (TPR)/sensitivity, and True Negative Rate (TNR)/specificity) evaluating the performance of both predictive models corroborate the results above (Fig. 10). The balanced accuracy for the all-variable predictive model (i.e., model 6: median = ~92.5%, 94.0%, 94.5%; Fig. 10) is noticeably greater than that of the mean predictive model (i.e., model 1: median = ~88.5%, 89.0%, 90.0%; Fig. 10) for the 40%, 60%, and 80% buffers, respectively. Likewise, the TPR and the TNR were also greater in the all-variable predictive model (median TPR: ~87.0%, 92.5%, 94.0%; median TNR: ~87.0%, 96.0%, 94.0%; Fig.10) than in that of the mean model (median TPR: ~84.0%, 87.5%, 88.0%; median TNR: ~84.5%, 91.5%, 93.0%; Fig. 10) for the 40%, 60%, and 80% buffers, respectively. Precision metrics for both predictive models generally increased in accuracy with increasing buffer sizes.

The predictive model with the least spatial autocorrelation in the residuals for *A. cognatus* was model 6. Incorporating climate heterogeneity within-geographic supercells and local spatial autocorrelation of the mean climate (i.e., SD of the bioclim variables and LSA of the mean bioclim variables, respectively) with the standard inclusion of climate heterogeneity between-geographic supercells (mean bioclimatic variables) effectively removed residual spatial autocorrelation, whereas it was still present under just the mean model (Fig. 11). This reduction in spatial autocorrelation in model 6 was further achieved with increasing buffer size. This was also true in the mean predictive model; spatial autocorrelation in the residuals reduced as a function of increasing buffer size.

DISCUSSION

Through this study, we demonstrate for the first time the importance of including the spatial structure of climate, such as climate heterogeneity (within-cell) and climate local spatial autocorrelation as predictors in species distribution models. We evaluated six different models testing both the individual and combined effects of various types of climate variables (i.e., climate heterogeneity among supercells (Mean), climate heterogeneity within supercells (SD), and climate local spatial autocorrelation (LSA)) on species distributions. This allowed us to explore the relative contributions of these predictors to model fit, the estimation of model coefficients, explaining species responses, and to predicting the probability of presence in the species *Anaxyrus* cognatus. As a very large number of biodiversity analyses test specific ecological hypotheses of interest and produce forecasting models based on fitting statistical relationships (see Guisan and Thuiller 2005), our results clearly demonstrate that our new class of predictors should always be considered in these analyses and models. Beyond demonstrating their relevance, our proposed predictors are particularly straightforward to implement. As such, our models are also practical in the sense that they can be readily implemented by biodiversity researchers, managers, and conservation planners.

General remarks on model performance and comparison

Across the 301 amphibian species evaluated, we found that, contrarily to our predictions (see Introduction), a model including all climate predictors (i.e., Mean + SD + LSA) did not always best explain the distributions of species in North America. However, it did for several species. There are a few potential explanations for this. The first, is statistical in nature; 154 species had a small number of occurrences (i.e., below 50) and of these, 55 had less than five occurrences. Though we compensated for this by both generating a greater proportion of pseudo-absences to actual presences and resampling additional occurrences from already existing ones, we obtained results for these species using data that were deficient in terms of sample sizes. This can lead to low statistical power and Type II error (Button et al. 2013). Ultimately, this affects our ability to correctly state whether the results obtained for these low occurring species corroborates or not our predictions, as the results may be due to chance alone (Colquhoun 2014).

The following two explanations are more ecological in nature; for the 20 out of 301 amphibian species having many occurrences (i.e., over 900), a model including all climate

predictors (i.e., model 6; see Methods) may not have better explained the response in their distributions because their realized niche may already be explained by the range of their occurrences. That is, they are at equilibrium with climate as they occur in all possible climatically suitable habitats and are, therefore, absent from those that are not (Araújo et al. 2005). Thus, for these species, it is not expected that the addition of spatial climatic predictors to the model explain their distributions better than the SDM using only the standard bioclimatic variables (i.e., climate heterogeneity among supercells) as model parameters. This is because these standard bioclimatic variables already sufficiently explain the climatic conditions governing their distributions (Araújo et al. 2005). The next explanation naturally pertains to species lying somewhere in between, with not too few but not too many occurrences. Each of these individual species responds differently to the climatic landscape. For some amphibian species, such as those with no distributional responses to climate heterogeneity and spatial structure, local-scale environmental heterogeneity may be what governs species richness (Couto et al. 2016). Thus, it is possible that the distributions and assemblages of these species are not influenced by broad-scale spatial structure in climate (such as climate heterogeneity within cells and climate local spatial autocorrelation). To this end, it may be more appropriate to consider spatial climatic predictors at the local scale (i.e., on the basis of microclimate) to evaluate their relative contributions to species distributions at fine spatial scales (Dufour et al. 2006; Couto et al. 2016). This is especially true when considering the body size, dispersal capacity, and thermal regulatory ability of the species or taxonomic group in question (Dufour et al. 2006; but see Pincebourde et al. 2016). In particular, we might expect the distributions of these amphibians to be more affected by climatic variation at fine spatial scales because they may have stronger dispersal limitations (e.g. strong dependence on moisture, aquatic life history or adult phase) and/or a strong reliance to specific climatic/environmental conditions (Provete et al. 2013; Couto et al. 2016; Pincebourde et al. 2016). In a similar vein, we might then expect that terrestrial species in general that have dispersal limitations and that are constrained to particular environmental features (e.g., a marsh, prairie grasslands) be more sensitive to spatial climatic processes at fine spatial scales than at broad spatial scales (Pincebourde et al. 2016). Even though our framework of utilizing climate spatial structure is clearly not applicable to all species, it has proven to be important to many. This was not always the case for most species with the model based on all climate predictors (i.e., Mean, SD, and LSA; model 6) at once. However, utilizing any of the spatial climatic variables (i.e., SD or LSA of climate) alone (i.e., models 2 and 3) or in

combination (models 4 and 5) with climate heterogeneity among supercells (i.e., mean bioclim variables), has demonstrated to be substantial in model performance and coefficient estimation, and most importantly, in explaining the distributions of species via model performance (i.e., AIC) (see Fig. 4; Table 1). In particular, the model uniquely utilizing local spatial autocorrelation of climate (i.e., model 3) was ranked as the best fitted model in a larger proportion of species than any other model. This was consistent across all buffer sizes and under both scenarios evaluated (see methods and see Fig. 4; Table 1). In fact, trends observed in species responses under the scenario including all 301 species were amplified under scenario 2 (i.e., species having between 50 and 900 occurrences), because we accounted for possible loss in statistical power and increased Type II errors by removing species with less than 50 and more than 900 occurrences (i.e., scenario 2; removing small sample sizes) (Button et al. 2013). For instance, under the 60% buffer in scenario 1, ~10% of species ranked model 6 as the best fitted model. This was slightly accentuated under scenario 2, where ~11% of species ranked model 6 as the best fitted model (see Fig. 4; Table 1). This trend was better emphasized and evermore impressive for model 3 (LSA of mean bioclim variables), where under the same buffer for scenario 1, this model ranked as the best fitted model in ~33.9% of species, and in scenario 2, it ranked as the best fitted model in ~38.6% of species.

Just for comparison, the standard SDM (i.e., model 1, mean of bioclimatic variables), ranked as the best-fitting model in only ~ 19.3% and 19.7 % of species under the same 60% buffer for scenarios 1 and 2, respectively. Had the spatial climate metrics (i.e., SD and LSA) utilized here not been important in explaining species distributions, then we would have expected poor model performance in these metrics across species. Along that same vein, we would then have also expected that the standard SDM (i.e., model 1) have the best overall performance across species. But that simply was not the case. Essentially, every spatial climate parameter applied in this study improved model performance for at least one species. The fact that model 1 did not actually rank as the first and alternated between being the second or third-best performing model demonstrates the importance of always considering models based on the new classes of proposed predictors (i.e., heterogeneity within geographic supercells and local spatial autocorrelation) in addition to the standard climate predictors (i.e., heterogeneity across geographic supercells).

Within-model coefficients

In the analysis ranking the coefficient estimates within-model across all iterations for all species, specifically for model 6 containing all classes of predictors, we observed that many of the coefficients that were ranked in species as having the most important contributions to their respective distributions were not uniquely attributed to predictors of the mean bioclim variables (i.e., predictors for climate heterogeneity among supercells) (see Fig.5; Fig. 6; Fig.7; Fig. 8). This is especially evident in the heatmap for all species (see Fig. 8) where, firstly, the highest ranked (e.g., top 10) predictors are a combination of the Mean, SD, and LSA of the climate. Secondly, there are numerous and large clusters of species in which the coefficients of these different predictors (i.e., Mean, SD, and LSA) were ranked as having the highest log-odds (i.e., probability) in explaining their distributions on the continent of North America. In essence, this means that the mean bioclim variables alone were not sufficient in predicting the distribution of a given species, further corroborating the importance of including additional spatial predictors of climate in SDMs (see *General remarks on model performance and comparison* section).

Furthermore, it is not unexpected that some individual predictors (e.g., mean 14 (i.e., precipitation of the driest month), SD 11 (i.e., mean temperature of the coldest quarter), LSA 7 (i.e., temperature annual range)) of each climate parameter evaluated cause stronger or weaker responses in each species, as evident by the cluster response of species to particular predictors (see Fig. 8). Species vary in their responses due to their individual ecological requirements, dispersal capacity, and life history (Büchi et al. 2009; Jimenez and Ricklefs 2014; Katayama et al. 2014; Provete et al. 2014; Pincebourde et al. 2016; Joly 2019; Guan et al. 2020). For instance, this would be akin to two species (*X* and *Y*) of frogs inhabiting a same landscape, where the distribution of species *X* is more affected by the heterogeneity of the temperature gradient within its habitat (i.e., SD of climate) than species *Y*. In the case of species *Y*, its distribution is more affected by the scattering of proximate and stably warm temperatures (i.e., LSA of climate) than that of species *X* (see Guan et al. 2020). However, though a given individual or a set of given individual predictors may explain the distribution of a given species better than others, it would be difficult to disentangle their effect without knowing their individual contributions and roles to the distribution of this species *a priori*. As such, we argue that it still be important to consider all bioclimatic variables rather than choose them selectively or arbitrarily. The evidence for this is derived from our

observations of the overall effect of each group (i.e., mean, SD, and LSA of the climate) of predictors. When taken altogether as a group of predictors of a same type (see Fig. 7), we observed that the overall effect of each group in general was important, at least in part, in explaining species' distributions across all 301 species.

Predictive models and residual spatial autocorrelation

To further illustrate the relevance of the new class of predictors that we are proposing, we selected a species (*Anaxyrus cognatus*) for which the inclusion of all spatial climate parameters (i.e., model 6) were important in its predictive model of the probability of presence. As discussed above (see Results and *General remarks on model performance and comparison* section of the Discussion), model 6 was not ranked as the model that performed best in most species. However, for some it was, and the Great Plains toad was one such species in which the inclusion of spatial parameters of climate greatly improved model predictions, as compared to just using the standard bioclimatic variables used in SDMs (i.e., between-patch climate heterogeneity) (see Fig. 9; Fig. 10). Evidence in selecting the model with all classes of predictors (i.e., model 6) as the best predictive model may lie in the possibility that the mean predictive model (i.e., model 1) was not sensitive enough (because of the nature of the arithmetic mean) in detecting or identifying any underlying signals or trends in the variation of climate values across geographic supercells for which *A. cognatus* was recorded as absent. However, by including other spatial climate metrics that were more sensitive to the latter, it made for a model that was more robust in detecting possible suitable or unsuitable climate patches in which the species could occur. In fact, when visually comparing the two predictive models (Fig. 9), not only are the overpredicted probability of presence values in the north-western corner of North America absent from the all-variable predictive model, but the uncertainty around all the predictions in its probabilities of presence is significantly reduced as well. Again, this further corroborates the importance of not only between-patch climate heterogeneity in improving the certainty and accuracy of this models' (i.e., model 6) predicted values for this species, but also climate heterogeneity within geographic supercells and climate local spatial autocorrelation (LSA).

The latter was only further supported by metrics evaluating model performance, such as balanced accuracy, the True Positive Rate (TPR) and the True Negative Rate (TNR) (see Introduction and Results; Fig. 10). In all of these, the all-variable predictive model outperformed

the mean predictive model. There were very clear differences between the performances of both models; in the mean predictive model, most values across all performance metrics fell between ~84% to 93%, whereas values in the performance metrics for the all-variable predictive model fell between ~87% to 96%. Moreover, after evaluating spatial autocorrelation in the model residuals of both predictive models, we observed that, unsurprisingly to the results in the predicted probabilities of presence, the mean predicted model had both positive and negative spatial autocorrelation in its model residuals (see Fig. 11). This was less apparent in the all-variable predictive model where there were only trace amounts of both negative and positive spatial autocorrelation in its model residuals. Seeing as how the residuals of both predictive models are still spatially autocorrelated (as dismal as it may be in the case of the all-variable predictive model), however, further spatial analyses are encouraged to account for this. One of many possibilities and possible future applications of our framework is to mitigate this using spatial eigenfunction analysis with a variation partitioning scheme (Grifith and Peres-Neto 2006; Legendre and Legendre 2012). These such methods are being increasingly employed in the ecological literature to reduce spatial autocorrelation that is common to ecological community data (Griffith and Peres-Neto 2006; Legendre and Legendre 2012).

Ecological significance

Our goal was to evaluate whether or not climate heterogeneity and climate spatial structure affect and contribute to the distributions of North American amphibian species. Our results demonstrate that spatial climatic processes such as climate heterogeneity (within and among geographic cells), and more specifically climate spatial structure, are important mechanisms underlying and modulating species distributions. Because the model using only climate local spatial autocorrelation (climate spatial structure) had the best fit in ~34% - 39% of species, it thus demonstrates its importance in explaining the current distributions of these species. Because our framework is very technical, in that it was a bulk analysis evaluating the responses of 301 amphibian species to spatial climatic processes, we did not specifically evaluate the relationship between these spatial climatic processes and species-specific characteristics, such as niche-breadth, dispersal capacity, life history, environmental preferences (e.g., wetlands, forests.), etc. However, based on the mechanisms of environmental heterogeneity and environmental spatial structure in structuring ecological communities and species distributions (see Introduction), we expect similar

outcomes from spatial climatic processes. Namely, we would expect that species with strong dispersal capacities and wide niche-breadths have broad distributions in landscapes with weak climate spatial structure. They are generally more resistant to strong variations in climatic conditions which would otherwise render dispersal corridors for their dispersal-limited and narrow niche-breadth counterparts as being impassable (Büchi and Vuilleumier 2014; Donelle 2018). As a result, dispersal-limited species and species with narrow niche-breadths may not even be able to occur under these types of climatic conditions, and therefore, would have either very small distributions, or none at all. Because strong dispersers and species with wide niche breadths are not being outcompeted (by their counterparts who are stronger competitors in landscapes with strong climate spatial structure) in landscapes with weak climate spatial structure, they benefit from the availability of multiple habitat types, which allows them to have broad distributions (Büchi and Vuilleumier 2012; Büchi and Vuilleumier 2014; Donelle 2018). In landscapes with strong climate spatial structure, we might also expect the distributions of species with strong dispersal capacities and wide-niche breadths to be large enough to broadly encompass those of species with limited dispersal capacities and narrow-niche breaths. This is because they must seek refuge in sites with less desirable climatic conditions where their counter parts are absent. Lastly, we might also expect species with poor dispersal capacities and narrow niche-breadths to have small distributions that somewhat but not completely overlap one another in landscapes with strong climate spatial structures. This is because for them to persist, they must partition their climatic environment to coexist with one another (Donelle 2018).

A note on buffer size in SDMs

Our results demonstrate an important observation in the choice of buffer size used when sampling background data for the purposes of species distribution models; it is parameter warranting further attention. Though the goal of our study was not to specifically evaluate the effect of buffer size on model performance and fit, coefficient estimation, and prediction accuracy, we noticed that there were obvious and consistent trends between the latter and increasing buffer size (or the extent of the study region utilizing in pseudo-absence sampling). Few studies have specifically evaluated the effect of buffer size on model fit, performance, and prediction (Anderson and Raza 2010; but see Barve et al. 2011). However, we observed generally, that the medians in ranked model fit (AIC) across species decrease with increasing buffer size (see Fig. 3). We also

observed that patterns in species distributions (e.g., through our heatmap of the ranked coefficients among species; Fig. 8) and in the percentage of species in which certain models fit better than others (see Fig. 4) were amplified with increasing buffer size. This was particularly evident for our case study of *A. cognatus*, where the predictions of the probability of presence and metrics measuring the performance of both predictive models typically improved in accuracy with increasing buffer size as well. Not only were these signals more acute with increasing buffer size, but there also appeared to be less uncertainty in the results. We do not have any premise on which to support these findings in the current study, as this was not the goal of our paper. Specifically, further research as to the effects of various buffer sizes used in SDMs on metrics such as the True Skill Statistic (TSS), Area Under the Operator-Receiving Curve (AUC-ROC), Akaike Information Criterion, and performance (e.g., True Positive Rate, True Negative Rate, False Positive Rate, False Negative Rate, and balanced accuracy) of prediction models could provide some interesting avenues of exploration on the topic. As it stands, current research in SDMs does not provide support for the arbitrary selection of buffer size, nor any explanation for the possible consequence of using the selected buffer size on the results (e.g., Warren et al. 2021). A solid foundation has already been laid on this topic by Barve et al. (2011) and to some degree, Anderson and Raza (2010), but a lot more work is needed to fully understand the implications of our choice of buffer size on sampling pseudo-absences using presence-only data for SDMs.

CONCLUSION

We argue that even if a model considering all classes of predictors were not the best model across all species, we provide critical evidence that their usage become general practice when fitting and ranking different SDMs for the same species. We can only know if the species or multiple species under study are affected by spatial variability and patterns in climate by testing their effects and evaluating their relative contributions in explaining the distributional responses of species to climate. Furthermore, we should evaluate how and whether different predictors covary (i.e., spatial autocorrelation) and if they improve model predictability (Peres-Neto and Legendre 2010; Monteiro et al. 2017); the subject of which would be important in future explorations and applications in the use of our framework in species distribution modelling. Future applications of our proposed framework could also explore the effects of other combinations of spatial climate

parameters (i.e., such as models 2, 3, 4, and 5) on the predictions of the probability of presence in other species, as a way of firstly, understanding the contributions of these explanatory variables to the predictions of a given species, and secondly, contrasting the predictions of each against one another and selecting the most parsimonious model. Another venue is to use standard model selection procedures (e.g., LASSO) even though they may bias our understanding of variable importance (Nathans et al. 2012).

Lastly, our framework also has important implications in conservation. Here, were demonstrated through a case study, that the novel inclusion of within-patch climate heterogeneity and climate local spatial autocorrelation are important spatial climatic parameters that improve the performance and accuracy of predictive models in the predictions of the probability of presence in the Great Plains toad (*Anaxyrus cognatus*). Moreover, inclusion of these parameters even decreased residual spatial autocorrelation in the predictive model. Our study thus establishes that our standard inclusion of climate heterogeneity among geographic cells in SDMs may not be accurately predicting suitable localities in which a species of interest may be found or possibly disperse to in the future. Therefore, in the best interest of conserving species and allocating financial resources to their conservation, as well as improving our understanding of species distributions in a spatial context, our framework should be considered in future species distribution model applications.

REFERENCES

Ai, D., D. Gravel, C. Chu, and G. Wang. 2013. Spatial structures of environment and of dispersal impact species distribution in competitive metacommunities. PLoS one **8**:e68927.

Akaike, H. 1974. A new look at the statistical model identification. IEEE Transactions on Automatic Control **19**(6):716–723.

Alford, R. A., and S. J. Richards. 1999. Global amphibian declines: a problem in applied ecology. Annual Review of Ecology and Systematics **30**:133-165.

Anderson, R.P. and A. Raza. 2010. The effect of the extent of the study region on GIS models of species geographic distributions and estimates of niche evolution: preliminary tests with montane rodents (genus *Nephelomys*) in Venezuela. Journal of Biogeography **37**: 1378-1393.

Anselin, L. 1995. Local Indicators of Spatial Association—LISA. Geographical Analysis **27**(2):93–115.

Araújo, K. C., A. Guzzi, and R. Avila. 2018. Influence of habitat heterogeneity on anuran diversity in Restinga landscapes of the Parnaíba River delta, northeastern Brazil. ZooKeys **757**:69–83.

Araújo, M. B., R. P. Anderson, A. M. Barbosa, C. M. Beale, C. F. Dormann, R. Early, R. A. Garcia, A. Guisan, L. Maiorano, B. Naimi, R. B. O'Hara, N. E. Zimmermann, and C. Rahbek. 2019. Standards for distribution models in biodiversity assessments. Science Advances **5**:eaat4858.

Araújo, M. B., and R. G. Pearson. 2005. Equilibrium of species' distributions with climate. Ecography **28**:693–695.

Araújo, M.B., R. G. Pearson, W. Thuiller, and M. Erhard. 2005. Validation of species-climate impact models under climate change. Global Change Biology **11**:1504–1513.

Barve, N., V. Barve, A. Jiménez-Valverde, A. Lira-Noriega, S. P. Maher, A. T. Peterson, J. Soberón, and F. Villalobos. 2011. The crucial role of accessible area in ecological niche modeling and species distribution modeling. Ecological Modelling **222**:1810-1819.

Basile, M., F. Valerio, R. Balestrieri, M. Posillico, R. Bucci, T. Altea, B. De Cinti, and G. Matteucci. 2016. Patchiness of forest landscape can predict species distribution better than abundance: the case of a forest-dwelling passerine, the short-toed treecreeper, in central Italy. PeerJ **4**:e2398.

Beisner, B. E., P. R. Peres-Neto, E. S. Lindström, A. Barnett, and M. L. Longhi. 2006. The role of environmental and spatial processes in structuring lake communities from bacteria to fish. Ecology **87**:2985–2991.

Ben-Hur, E., and R. Kadmon. 2020. An experimental test of the area-heterogeneity tradeoff. Proceedings of the National Academy of Sciences **117**:4815–4822.

Bishop, P. J., A. Angulo, J. P. Lewis. R. D. Moore, G. B. Rabb, and J. Garcia. 2012. The amphibian extinction crisis – what will it take to put the action into the Amphibian Conservation Action Plan? Surveys and Perspectives Integrating Environment and Society [accessed November 1st, 2021]; **5** (IUCN Commissions).

Biswas, S. R., R. L. MacDonald, and H. Y. H. Chen. 2017. Disturbance increases negative spatial autocorrelation in species diversity. Landscape Ecology **32**(823-834).

Bonebrake, T. C., and C. A. Deutsch. 2012. Climate heterogeneity modulates impact of warming on tropical insects. Ecology **93**:449–455.

Boone, M. D., P. S. Corn, M. A. Donnelly, E. E. Little, and P. H. Niewiarowski. 2003. Physical stressors. In: Linder G. L., Krest, S.K., Sparling D. W, editors. Amphibian decline: an integrated analysis of multiple stressor effects. Pensacola, Florida: SETAC. p.129-151.

Brodman, R. 2009. A 14-year study of amphibian populations and metacommunities. Herpetological Conservation and Biology **4**:106-119.

Büchi, L., P-A. Christin, and A. H. Hirzel. 2009. The influence of environmental spatial structure on the life-history traits and diversity of species in a metacommunity. Ecological Modelling **220**:2857-2864.

Büchi, L., and S. Vuilleumier. 2012. Dispersal strategies, few dominating or many coexisting: the effect of environmental spatial structure and multiple sources of mortality. PLoS one **7**:e34733.

Büchi, L. and Vuilleumier. 2014. Coexistence of specialist and generalist species is shaped by dispersal and environmental factors. The American Naturalist **183**:612-624.

Button K. S., J. P. A. Ioannidis, C. Mokrysz, B. A. Nosek, J. Flint, E. S. J. Robinson, and M. R. Munafò. 2013. Power failure: why small sample size undermines the reliability of neuroscience. Nature Reviews **14**:365-376.

Catenazzi, A. 2015. State of the world's amphibians. Annual Review of Environment and Resources **40**:91-119.

Catford, J. A., J. R. U. Wilson, P. Pyšek, P. E. Hulme, and R. R. Duncan. 2021. Addressing context dependency in ecology. Trends in Ecology and Evolution **2914**:1-13.

Chesson, P. 2000. General theory of competitive coexistence in spatially-varying environments. Theoretical Population Biology **58**:211–237.

Choi, W., R. Tareghian, J. Choi, and C. Hwang. 2014. Geographically heterogeneous temporal trends of extreme precipitation in Wisconsin, USA during 1950-2006. International Journal of Climatology **34**:2841–2852.

Cohen, J. M., D. J. Civitello, A. J. Brace, E. M. Feichtinger, C. N. Ortega, J. C. Richardson, E. L. Sauer, X. Liu, and J. R. Rohr. 2016. Spatial scale modulates the strength of ecological processes driving disease distributions. Proceedings of the National Academy of Sciences **113**: E359-E364.

Colquhoun, D. 2014. An investigation of the false discovery rate and the misinterpretation of *p*-values. The Royal Society of Open Science **1**:140216.

Corn, P. S. 2005. Climate change and amphibians. Animal Biodiversity and Conservation **28**:59-67.

Cornell, H. V., and J. H. Lawton. 1992. Species interactions, local and regional processes, and limits to the richness of ecological communities: a theoretical perspective. Journal of Animal Ecology **61**:1-12

Costa, G. C., C. Nogueira, R. B. Machado, and G. R. Colli. 2007. Squamate richness in the Brazilian Cerrado and its environmental-climatic associations. Diversity and Distributions **13**: 714-724.

Cottenie K. 2005. Integrating environmental and spatial processes in ecological community dynamics: meta-analysis of metacommunities. Ecology Letters **8**:1175–1182.

Couto, A. P., E. Ferreira, R. T. Torres, and C. Fonseca. 2017 Local and landscape drivers of pond-breeding amphibian diversity at the northern edge of the Mediterranean. Herpetologica **73**:10-17.

D'Amen, M., C. Rahbek, N. E. Zimmermann, and A. Guisan. 2017. Spatial predictions at the community level: from current approaches to future frameworks. Biological Reviews **92**:169-187.

Di Marco, M., J. E. M. Watson, H. P. Possingham, and O. Venter. 2017. Limitations and trade-offs in the use of species distribution maps for protected area planning. Journal of Applied Ecology **54**:402–411.

Diniz-Filho, J. A. F., and L. M. Bini. 2005. Modelling geographical patterns in species richness using eigenvector-based spatial filters: spatial filtering of richness data. Global Ecology and Biogeography **14**:177–185.

Diniz-Filho, J. A. F., L. M. Bini, C. M. Vieira, D. Blamires, L. C. Terribile, R. P. Bastos, G. de Oliveira, and B. de S. Barreto. 2008. Spatial patterns of terrestrial vertebrate species richness in the Brazilian Cerrado. Zoological Studies **47**:146-157.

Donelle, L. 2018. The effects of the spatial structure of the environment on species coexistence and related consequences to local and regional community structure. Montreal, Quebec, Canada: Concordia University.

Dormann, C. F., J. M. McPherson, M. B. Araújo, R. Bivand, J. Bolliger, G. Carl, R. Davies, A. Hirzel, W. Jetz, D. Kissling, I. Kühn, R. Ohlemüller, P. R. Peres-Neto, R. Björn, B. Schröder, F. M. Schurr, and R. Wilson. 2007. Methods to account for spatial autocorrelation in the analysis of species distributional data: a review. Ecography **30**:609-628.

Dray, S. 2011. A new perspective about Moran's coefficient: spatial autocorrelation as a linear regression problem. Geographical Analysis **43**:127-141.

Dufour, A., F. Gadallah, H. H. Wagner, A. Guisan, and A. Buttler. 2006. Plant species richness and environmental heterogeneity in a mountain landscape: effects of variability and spatial configuration. Ecography **29**:573–584.

Elith, J., and J. R. Leathwick. 2009. Species distribution models: ecological explanation and prediction across space and time. Annual Review of Ecology, Evolution, and Systematics **40**:677-697.

Esparza-Orozco, A., A. Lira-Noriega, J. F. Martínez-Montoya, L. F. Pineda-Martínez, and S de J. Méndez-Gallegos. 2020. Influences of environmental heterogeneity on amphibian composition at breeding sites in a semiarid region of Mexico. Journal of Arid Environments **182**:104259.

Ficetola, G. F., C. Rondinini, A. Bonardi, V. Katariya, E. Padoa-Schioppa, and A. Angulo. 2014. An evaluation of the robustness of global amphibian range maps. Journal of Biogeography **41**:211–221.

Fick, S. E., and R. J. Hijmans. 2017. WorldClim 2: new 1 km spatial resolution climate surfaces for global land areas. International Journal of Climatology **37**: 4302-4315.

Flater, D. 2011. Understanding geodesic buffering. URL: https://www.esri.com/news/arcuser/0111/geodesic.html [accessed on 17 May 2021].

Fortin, M-J., M. R. T. Dale, and J. M. ver Hoef. 2006. Spatial Analysis in Ecology. Encyclopedia of Environmetrics **4**:2051-2058.

Fortin, M-J., M. R. T. Dale, J. M. ver Hoef. 2013. Spatial Analysis in Ecology. In: El-Shaarawi, A. H., and Piegorsch W. W., editors. Encyclopedia of Environmetrics. Second Edition: John Wiley & Sons, Ltd.

Fournier, B., H. Vázquez-Rivera, S. Clappe, L. Donelle, P. H. P. Braga, and P. R. Peres-Neto. 2020. The spatial frequency of climatic conditions affects niche composition and functional diversity of species assemblages: the case of Angiosperms. Ecology Letters **23**:254–264.

Fu, W. J., P. K. Jiang, G. M. Zhou, and K. L. Zhao. 2014. Using Moran's I and GIS to study the spatial pattern of forest litter carbon density in a subtropical region of southeastern China. Biogeosciences **11**:2401–2409.

Fujiwara, M. and T. Takada. 2017. Environmental stochasticity. In: eLS. Chichester, United Kingdom: John Wiley & Sons, Ltd.

Garcia, R. A., M. Cabeza, C. Rahbek, and M. B. Araújo. 2014. Multiple dimensions of climate change and their implications for biodiversity. Science **344**:1247579.

Gelman, A., and J. Hill. 2007. Data analysis using regression and multilevel/hierarchical models. Cambridge, United Kingdom: Cambridge University Press.

Gelman, A., and Y-S. Su. 2016. arm: data analysis using regression and multilevel/hierarchical models. R package version 1.9-1. Retrieved from: https://CRAN.R-project.org/package=arm

Griffith, D. A., and P. R. Peres-Neto. 2006. Spatial modeling in ecology: the flexibility of eigenfunction spatial analyses. Ecology **87**:2603–2613.

Guan, Y., H. Lu, L. He, H. Adhikari, P. Pellikka, E. Maeda, and J. Heiskanen. 2020. Intensification of the dispersion of the global climatic landscape and its potential as a new climate change indicator. Environmental Research Letters **15**:114032.

Guan, Y., H. Lu, Y. Jiang, P. Tian, L. Qiu, P. Pellikka, and J. Heiskanen. 2021. Changes in global climate heterogeneity under the 21st century global warming. Ecological Indicators **130**:108075

Guerra, C., and E. Aráoz. 2015. Amphibian diversity increases in an heterogeneous agricultural landscape. Acta Oecologica **69**:78–86.

Guisan, A., and W. Thuiller. 2005. Predicting species distribution: offering more than simple habitat models. Ecology Letters **8**:993–1009.

Guisan, A., W. Thuiller, and N. E. Zimmermann. 2017. Habitat suitability and distribution models with applications in R. Cambridge, United Kingdom: Cambridge University Press.

Guisan, A., and N. E. Zimmermann. 2000. Predictive habitat distribution models in ecology. Ecological Modelling **135**:147-186.

Hand, D. J., and C. Anagnostopoulos. 2013. When is the area under the receiver operating characteristic curve an appropriate measure of classifier performance? Pattern Recognition Letters **34**:492-495.

Hefley, T. J., and M. B. Hooten. 2015. On the existence of maximum likelihood estimates for presence-only data. Methods in Ecology and Evolution **6**:648-655.

Herkt, K. M. B., A. K. Skidmore, and J. Fahr. 2017. Macroecological conclusions based on IUCN expert maps: a call for caution. Global Ecology and Biogeography **26**:930–941.

Hof, C. 2010. Species distributions and climate change: current patterns and future scenarios for biodiversity. Copenhagen, Denmark: University of Copenhagen.

Howard. S. D., and D. P. Bickford. 2014. Amphibians over the edge: silent extinction risk of data deficient species. Diversity and Distributions **20**: 837-846.

Hsiung, H-Y., B-H. Huang, J-T. Chang, Y-M. Huang, C-W. Huang, and P-C. Liao. 2017. Local climate heterogeneity shapes populations genetic structure of two undifferentiated insular *Scutellaria* species. Frontiers in Plant Science **8**:1–17.

Huang, Y., Q. Dai, Y. Chen, H. Wan, J. Li, and Y. Wang. 2011. Lizard species richness patterns in China and its environmental associations. Biodiversity and Conservation **20**:1399–1414.

Hutchinson, G. E. 1957. Concluding remarks. Cold Spring Harbor Symposia on Quantitative Biology **22**:415-427.

IUCN 2018. The IUCN Red List of Threatened Species. Version 2020-3. https://www.iucnredlist.org. Downloaded on [16 July 2018].

Jarvie, S., and J-C. Svenning. 2018. Using species distribution modelling to determine opportunities for trophic rewilding under future scenarios of climate change. Philosophical Transactions of the Royal Society B: Biological Sciences **373**:20170446.

Jimenez, I., and R. E. Ricklefs. 2014. Diversity anomalies and spatial climate heterogeneity. Global Ecology and Biogeography **23**:988–999.

Joly, P. 2019. Behavior in a changing landscape: using movement ecology to inform the conservation of pond-breeding amphibians. Frontiers in Ecology and Evolution **7**:155.

Katayama, N., T. Amano, S. Naoe, T. Yamakita, I. Komatsu, S. Takagawa, M. Ueta, and T. Miyashita. 2014. Landscape heterogeneity–biodiversity relationship: effect of range size. PLoS one **9**:e93359.

Kassen, R. 2002. The experimental evolution of specialists generalists, and the maintenance of diversity. Journal of Evolutionary Biology **15**: 173-190.

Keller, A., M-O. Rodel, K. E. Linsenmair, and T. U. Grafe. 2009. The importance of environmental heterogeneity for species diversity and assemblage structure in Bornean stream frogs. Journal of Animal Ecology **78**:305–314.

Kumar, M., H. Padalia, S. Nandy, H. Singh, P. Khaiter, and N. Kalra. 2019. Does spatial heterogeneity of landscape explain the process of plant invasion? A case study of *Hyptis suaveolens* from Indian Western Himalaya. Environmental Monitoring and Assessment **191**:794.

Landeiro, V. L., F. Waldez, and M. Menin. 2014. Spatial and environmental patterns of Amazonian anurans: differences between assemblages with aquatic and terrestrial reproduction, and implications for conservation management. Natureza & Conservação **12**:42–46.

Lannoo, M. 2005. Amphibian declines. London, England: University of California Press.

Legendre, P. 1993. Spatial Autocorrelation: trouble or new paradigm? Ecology **74**:1659–1673.

Legendre, P., and L. Legendre. 2012. Chapter 14: Multiscale analysis: spatial eigenfunctions. In: P. Legendre, L. Legendre, editors. Numerical Ecology. Oxford, United Kingdom: Elsevier. p.859-906.

Legendre, P., D. Borcard, and P. R. Peres-Neto. 2005. Analyzing beta diversity: partitioning the spatial variation of community composition data. Ecological Monographs **75**:435-450.

Leibold, M. A., and J. M. Chase. 2018. Metacommunity ecology. Princeton, New Jersey and Oxford, United Kingdom: Princeton University Press.

Leibold, M. A., M. Holyoak, N. Mouquet, P. Amarasekare, J. M. Chase, M. F. Hoopes, R. D. Holt, J. B. Shurin, R. Law, D. Tilman, M. Loreau, and A. Gonzalez. 2004. The metacommunity concept: a framework for multi-scale community ecology. Ecology Letters **7**:601–613.

Leibold, M. A., and M. A. McPeek. 2006. Coexistence of the niche and neutral perspectives in community ecology. Ecology **87**:1399–1410.

Leibold, M. A., F. J. Rudolph, F. G. Blanchet, L. De Meester, D. Gravel, F. Hartig, P. R. Peres-Neto, L. Shoemaker, and J. M. Chase. 2021. The internal structure of metacommunities. Oikos **00**:1-13.

Logue, J. B., N. Mouquet, H. Peter, and H. Hillebrand. 2011. Empirical approaches to metacommunities: a review and comparison with theory. Trends in Ecology & Evolution **26**:482–491.

Menge, B. A., and A. M. Olson. 1990. Role of scale and environmental factors in regulation of community structure. Trends in Ecology and Evolution **5**:52-57.

Mielke, K. P., T. Claassen, M. Busana, T. Heskes, M. A. J. Huijbregts, K. Koffijberg, and A. M. Schipper. 2020. Disentangling drivers of spatial autocorrelation in species distribution models. Ecography **43**:1741-1751.

Miller, D. A.W., E. H. C. Grant, E. Muths, S. M. Amburgey, M. J. Adams, M. B. Joseph, J. H. Waddle, P. T. J. Johnson, M. E. Ryan, B. R. Schmidt et al. 2018. Quantifying climate sensitivity and climate-driven change in North American amphibian communities. Nature Communications **9**: 3926.

Mittelbach, G. G., and D. W. Schemske. 2015. Ecological and evolutionary perspectives on community assembly. Trends in Ecology and Evolution **30**:241–247.

Monteiro, V. F., P. C. Paiva, and P. R. Peres-Neto. 2017. A quantitative framework to estimate the relative importance of environment, spatial variation and patch connectivity in driving community composition. Journal of Animal Ecology **86**:316–326.

Mouquet, N,. and M. Loreau. 2002. Coexistence in metacommunities: the regional similarity hypothesis. American Naturalist **159**:420–426.

Nathans, L.L., F. L. Oswald, and K. Nimon. 2012. Interpreting multiple linear regression: a guidebook of variable importance. Practical Assessment, Research & Evaluation **17**:1-19

Nenzén, H. K., and M. B. Araújo. 2011. Choice of threshold alters projections of species range shifts under climate change. Ecological Modelling **222**:3346-3354.

Olden, J. D., D. A. Jackson, and P. R. Peres-Neto. 2002. Predictive models of fish species distributions: a note on proper validation and chance predictions. Transactions of the American Fisheries Society **131**:329-336.

Orrock, J. L. 2020. Deterministic insights from stochastic interactions. Proceedings of the Natural Academy of Sciences **117**:6965–6967.

Ortiz-Yusty, C. E., V. Páez, and F. A. Zapta. 2013. Temperature and precipitation as predictors of species richness in northern Andean amphibians from Columbia. Caldasia **35**:65-80.

Osborne, P. E., G. M. Foody, and S. Suárez-Seoane. 2007. Non-stationarity and local approaches to modelling the distributions of wildlife. Diversity and Distributions **13**:313–323.

Palmer, M. W., and P. M. Dixon. 1990. Small-scale environmental heterogeneity and the analysis of species distributions along gradients. Journal of Vegetation Science **1**:57-65.

Pearson, R. G. and T. P. Dawson. 2003. Predicting the impacts of climate change on the distribution of species: are bioclimate envelope models useful? Global Ecology and Biogeography **12**:361-371.

Pebesma, E., 2018. Simple features for R: standardized support for spatial vector data. The R Journal **10**: 439-446.

Pebesma, E., and R. Bivand. 2005. Classes and methods for spatial data in R. R News **5**:9-13.

Peres-Neto, P. R., and P. Legendre. 2010. Estimating and controlling for spatial structure in the study of ecological communities. Global Ecology and Biogeography **19**:174–184.

Peres-Neto, P. R., M. A. Leibold, and S. Dray. 2012. Assessing the effects of spatial contingency and environmental filtering on metacommunity phylogenetics. Ecology **93**:S14–S30.

Perry, J. N., A. M. Leibhold, M. S. Rosenberg, J. Dungan, M. Miriti, A. Jakomulska, and S. Citron-Pousty. 2002. Illustrations and guidelines for selecting statistical methods for quantifying spatial pattern in ecological data. Ecography **25**:578–600.

Peterson, A. T., J. Soberón, R. G. Pearson, R. P. Anderson, E. Martínez-Meyer, and M. Nakamura. 2011. Ecological niches and geographic distributions (MPB-49). Princeton, New Jersey and Oxford, United Kingdom: Princeton University Press.

Pincebourde, S., C. C. Murdock, M. Vickers, and M. W. Sears. 2016. Fine-scale microclimatic variation can shape the responses of organisms to global change in both natural and urban Environments. Integrative and Comparative Biology **56**:45–61.

Presley, S. J., C. L. Higgins, and M. R. Willig. 2010. A comprehensive framework for the evaluation of metacommunity structure. Oikos **119**:908–917.

Provete, D. B., T. Gonçalves-Souza, M. V. Garey, I. A. Martins, and D de C. Rossa-Feres. 2014. Broad-scale spatial patterns of canopy cover and pond morphology affect the structure of a Neotropical amphibian metacommunity. Hydrobiologia **734**:69–79.

Qian, H. 2010. Environment-richness relationships for mammals, birds, reptiles, and amphibians at global and regional scales. Ecological Research **25**:629-637.

Qian, H. X. Wang, S. Wang, and Y. Li. 2007. Environmental determinants of amphibian and reptile species richness in China. Ecography **30**: 471-482.

R Core Team. 2021. R: a language and environment for statistical computing. R Foundation for Statistical Computing, Vienna, Austria. URL:https://www.R-project.org/.

Record, S., M. C. Fitzpatrick, A. O. Finley, S. Veloz, and A. M. Ellison. 2013. Should species distribution models account for spatial autocorrelation? A test of model projections across eight millennia of climate change. Global Ecology and Biogeography **22**:760–771.

Ricklefs, R. E. 2004. A comprehensive framework for global patterns in biodiversity. Ecology Letters **7**:1–15.

Rodríguez, M.Á., J.A., Belmontes, and B. A., Hawkins. 2005. Energy, water and large-scale patterns of reptile and amphibian species richness in Europe. Acta Oecologica **28**:65-70.

Rojas-Ahumada, D. P., V. L. Landeiro, and M. Menin. 2012. Role of environmental and spatial processes in structuring anuran communities across a tropical rain forest. Austral Ecology **37**:865–873.

Sarkar, D. 2008. Lattice multivariate data visualization with R. New York, USA: Springer.

Shen, G., F. He, R. Waagepetersen, I-F. Sun, Z. Hao, Z-S. Chen, and M. Yu. 2013. Quantifying effects of habitat heterogeneity and other clustering processes on spatial distributions of tree species. Ecological Society of America **94**: 2436-2443.

Silva, R. A., I. A. Martins, and D de C. Rossa-Feres. 2011. Environmental heterogeneity: anuran diversity in homogeneous environments. Zoologia **28**:610–618.

Singh, V., and M. K. Goyal. 2016. Changes in climate extremes by the use of CMIP5 coupled climate models over eastern Himalayas. Environmental Earth Sciences **75**:839.

Smith, A., and D. M. Green. 2005. Dispersal and the metapopulation paradigm in amphibian ecology and conservation: are all amphibian populations metapopulations? Ecography **28**:110-128.

Smulders, M., T. A. Nelson, D. E. Jelinski, and S. E. Nielsen, and G. B. Stenhouse. 2010. A spatially explicit method for evaluating accuracy of species distribution models. Diversity and Distributions **16**:996–1008.

Stein, A., K. Gerstner, and H. Kreft. 2014. Environmental heterogeneity as a universal driver of species richness across taxa, biomes and spatial scales. Ecology Letters **17**:866–880.

Titley, M. A., J. L. Snaddon, and E. C. Turner. 2017. Scientific research on animal biodiversity is systematically biased towards vertebrates and temperate regions. PLoS one **12**: e0189577.

Tordoni, E., V. Casolo, G. Barcaro, F. Martini, A. Rossi, and F. Boscutti. 2020. Climate and landscape heterogeneity drive spatial pattern of endemic plant diversity within local hotspots in South-Eastern Alps. Perspectives in Plant Ecology, Evolution and Systematics **43**:125512.

Vellend, M. 2010. Conceptual synthesis in community ecology. The Quarterly Review of Biology **85**:183–206.

Warren, D. L., A. Dornburg, K. Zapfe, and T. L. Iglesias. 2021. The effects of climate change on Australia's only endemic Pokémon: Measuring bias in species distribution models. Methods in Ecology and Evolution **12**:985–995.

Wickham, H. 2016. ggplot2: elegant graphics for data analysis. New York, USA: Springer-Verlag.

Wind, E. 1999. Effects of habitat fragmentation on amphibians: what do we know and where do we go from here? Proceedings on the Biology and Management of Species and Habitats at Risk **2**:885-894.

Yuan, Y., M. Cave, and C. Zhang. 2018. Using Local Moran's I to identify contamination hotspots of rare earth elements in urban soils of London. Applied Geochemistry **88**:167–178.

Zhang, C., L. Luo, W. Xu, and V. Ledwith. 2008. Use of local Moran's I and GIS to identify pollution hotspots of Pb in urban soils of Galway, Ireland. Science of The Total Environment **398**:212–221.

Zhang, L., J. H. Gove, and L. S. Heath. 2005. Spatial residual analysis of six modeling techniques. Ecological Modelling **186**:154–177.

FIGURES

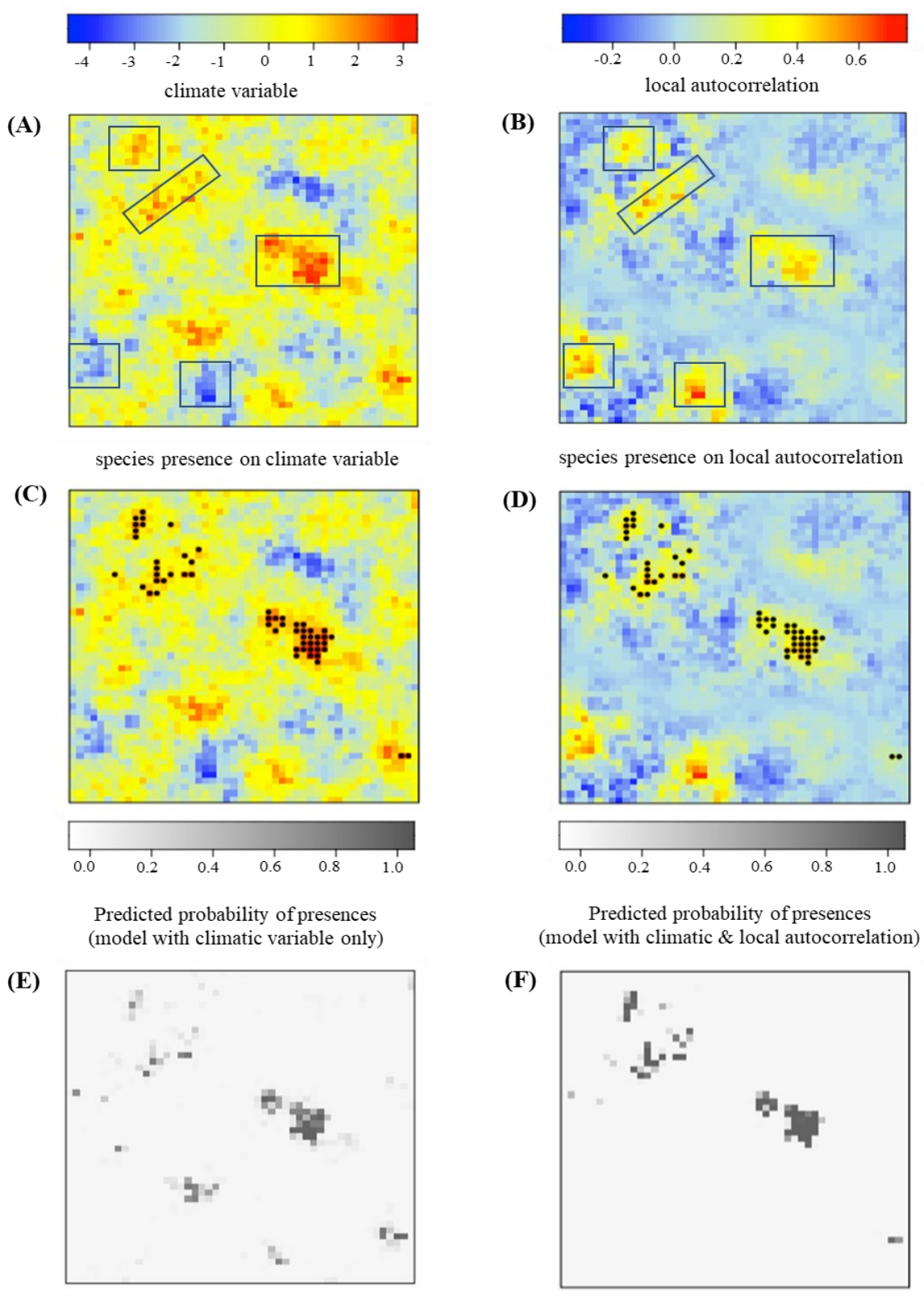
-4 -3 -2 -1 0 1 2 3
climate variable
-0.2 0.0 0.2 0.4 0.6
local autocorrelation
(A)
(B)
species presence on climate variable
species presence on local autocorrelation
(C)
(D)
0.0 0.2 0.4 0.6 0.8 1.0
Predicted probability of presences
(model with climatic variable only)
0.0 0.2 0.4 0.6 0.8 1.0
Predicted probability of presences
(model with climatic & local autocorrelation)
(E)
(F)

Figure 1. Fictional example of the proposed modelling framework for a landscape with 2500 patches (50 x 50 patches). This figure aims at facilitating the understanding of the proposed framework. **(A)** Map of a simulated climate variable (say average annual temperature) with an intermediate level of spatial autocorrelation. The zones within boxes represent large clusters of cells with similar temperatures that are relatively well isolated from other cell clusters with the same values. These clusters contain the cells with the largest local positive autocorrelation. **(B)** Map of local Moran's *I* of temperature. Note that local autocorrelation values (negative or positive) relate to large clusters of cells regardless of whether they have relatively lower (blue) or warmer (red) temperatures. Boxes represent areas of positive autocorrelation only to facilitate visualization. Because temperatures were generated to be positively autocorrelated over the entire landscape, most cells have a positive local autocorrelation; **(C)** Cells occupied (black dots) by a species simulated on the basis of climate and local spatial autocorrelation. Species presences are mapped on the climate variable; **(D)** Species presences of the simulated species on the map of local spatial autocorrelation. Note that the species is present in cells with both relatively warm temperatures (red) and relatively high local spatial autocorrelation. **(E)** Predicted values from a logistic regression using only temperature as predictor and **(F)** predicted values considering both temperature and local autocorrelation as predictors. The predicted values based on a model with temperature only (panel **A**) would obviously predict its presence (high probabilities) in relatively warm sites (i.e., cells). However, when considering a model with both temperature and local autocorrelation, it suggests that the species occupies only large clusters of cells with relatively warm temperatures (contrast panels **C**, **D** and **F**). Small cell clusters of relatively warm temperatures do not seem to be able to sustain the fictional species.

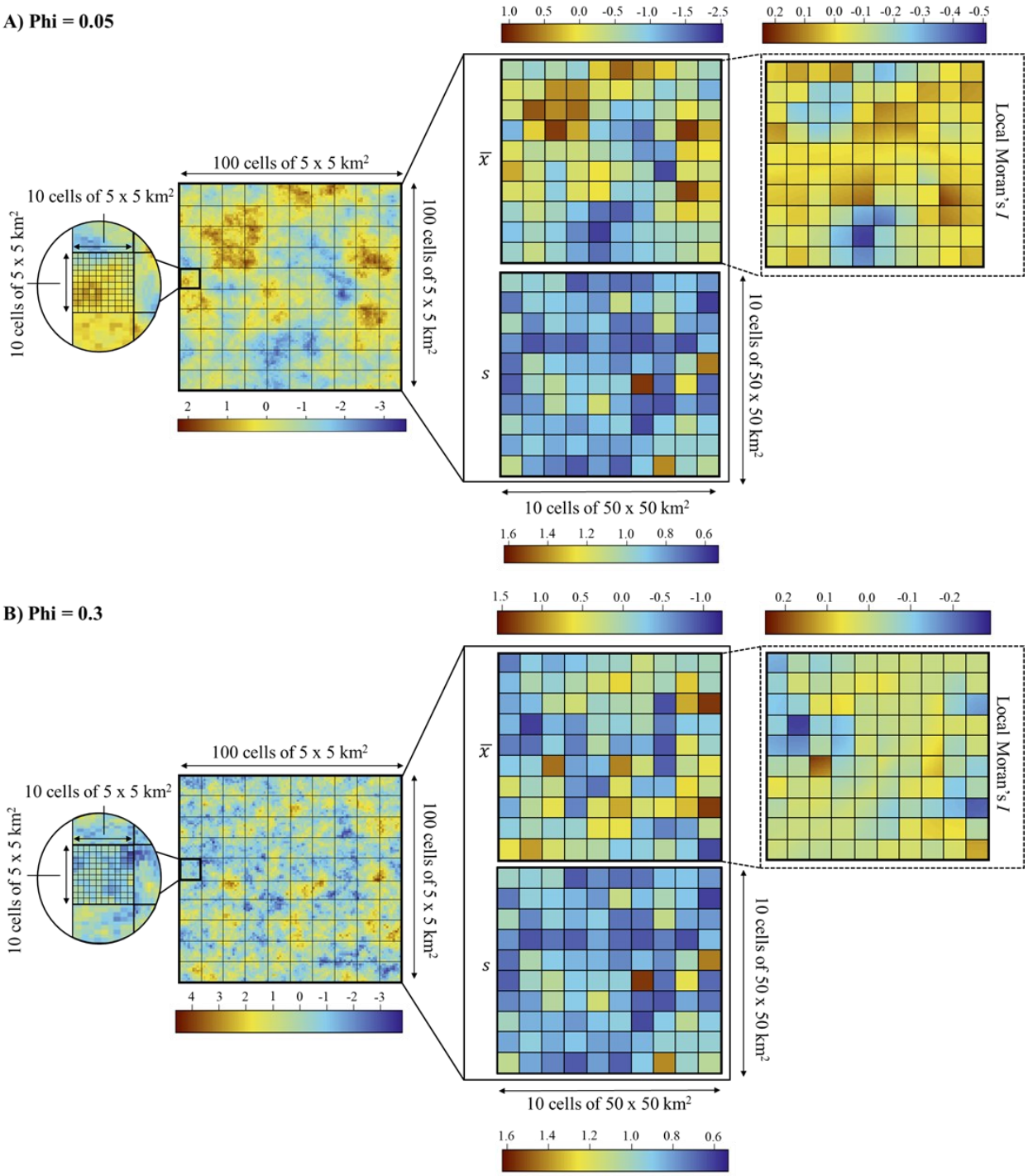

Figure 2: Illustration of the methodology for preparing the WorldClim climate data to calculate climate heterogeneity between geographic cells (Mean), climate heterogeneity within geographic cells SD, and local Moran's *I* (LSA). Spatial patterns were simulated using a spherical variogram model with mean zero and parameter phi = 0.05 (strong autocorrelation; panel **A**) and phi = 0.3 (intermediate autocorrelation; panel **B**). As in our study, the simulated landscape has geographic supercells of 50 x 50 km^2 (100 cells in total instead of the 7035 cells as in North America). Each geographic supercell (50 x 50 km^2) has climate values for 100 geographic cells of 5 x 5 km^2. Values for these 100 cells are used to calculate mean ($\bar{X}$) and standard

deviation s for each supercell. The variation in mean values represent environmental heterogeneity across cells (patches) whereas the standard deviation represents climate heterogeneity within cells (i.e., local heterogeneity). The mean values $\bar{X}$ are used to calculate local Moran's I (spatial structure of climate) for each geographic supercell.

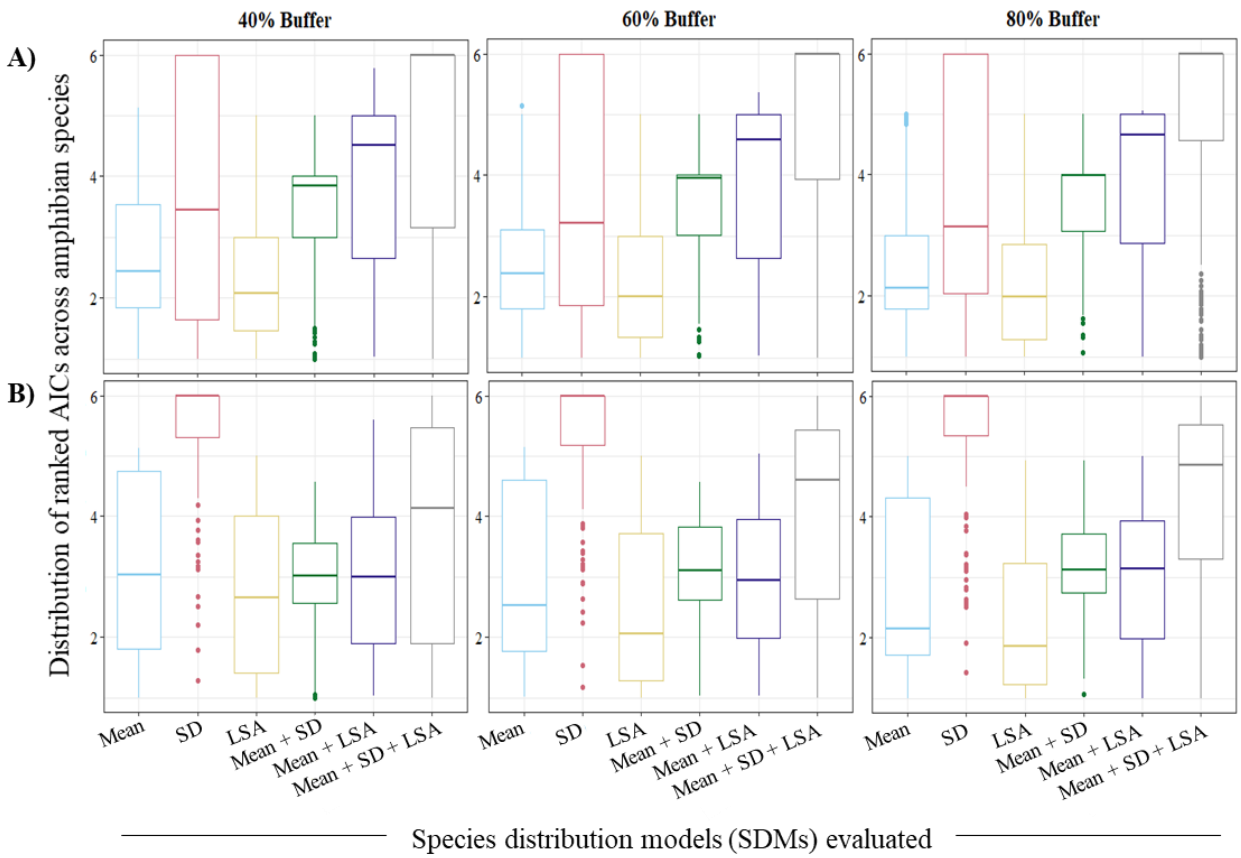

Figure 3: Ranked model fit (i.e., AIC) across amphibian species for all six species distribution model (SDM) specifications evaluated at different spatial scales for scenarios 1 (i.e., all 301 amphibian species) and 2 (i.e., 127 amphibian species having between 50 and 900 presences). Each species had 300 models (100 background data and three buffers) for each of the six SDM specifications. Model fit (i.e., AIC) was ranked for each of the 300 models for each species and for each SDM specification. The mean rank of each SDM specification over the 100 models for each buffer for each species was then calculated for (**A**) all 301 species (scenario 1) and (**B**) 127 species having between 50 and 900 occurrences (scenario 2). Rows **A** and **B** represent scenarios 1 and 2, respectively. Plot columns represent different spatial scales, where a given buffer size (i.e., 40%, 60%, and 80%, respectively) represents the radius (as a percentage of the maximum pairwise distances between a focal occurrence and each of its neighbours) within which background absences were sampled for species. Each SDM specification is colored accordingly for both scenarios and across all buffers, where blue = Mean model (i.e., model 1; between-patch climate heterogeneity), red = SD model (i.e., model 2; within-patch climate heterogeneity), yellow = SA model (i.e., model 3; climate local spatial autocorrelation), green = Mean + SD model (i.e., model 4; between-patch climate heterogeneity + within-patch climate heterogeneity), purple = Mean + LSA (i.e., model 5; between-patch climate heterogeneity + climate local spatial autocorrelation), and grey = Mean + SD + LSA (i.e., model 6; between-patch climate heterogeneity + within-patch climate heterogeneity + climate local spatial autocorrelation).

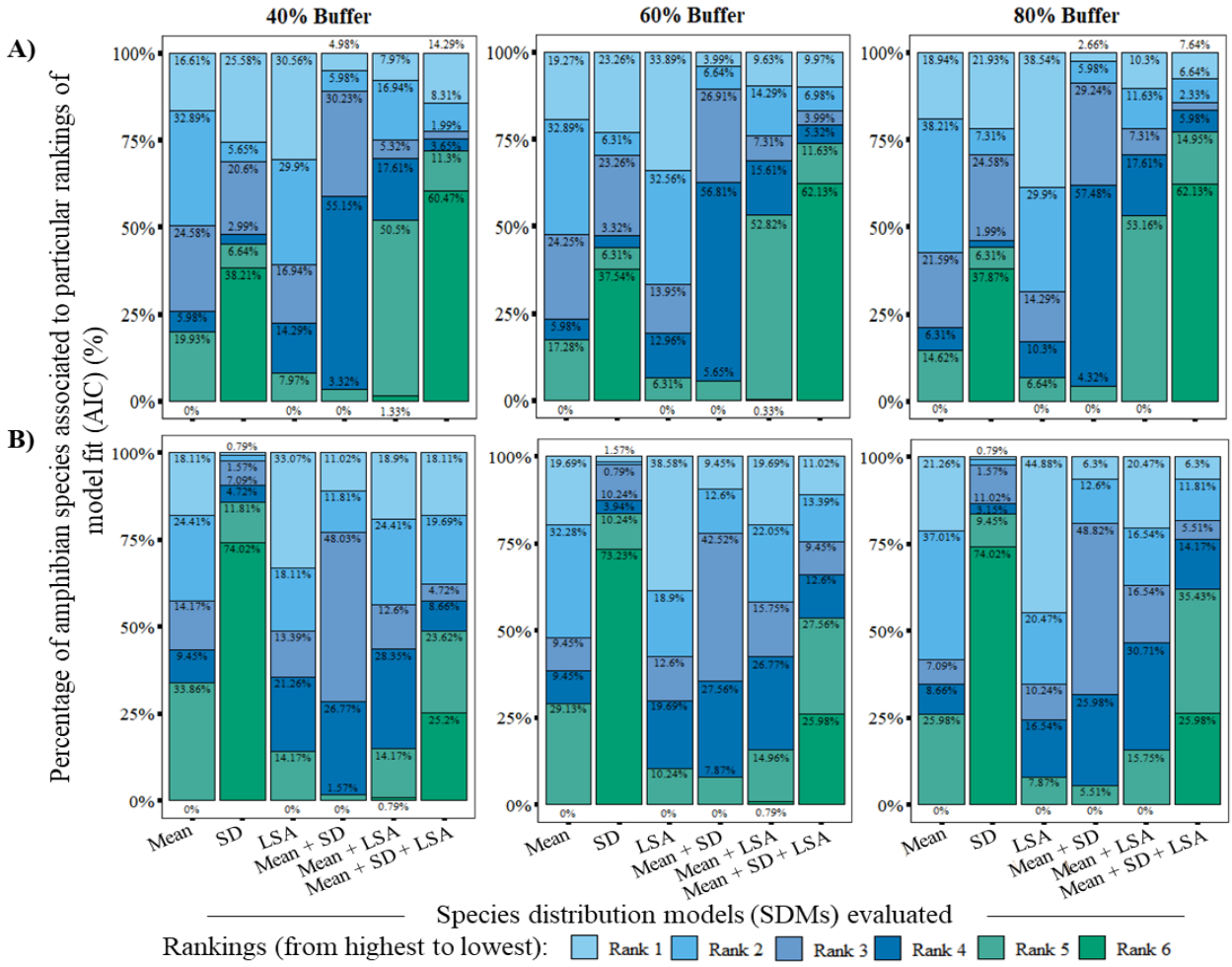

Figure 4: Proportion (in percentage) of species under scenarios 1 (all 301 species) and 2 (127 species having between 50 and 900 occurrences) associated to mean rankings of model fit (i.e., AIC) for each of the six species distribution model (SDM) specifications at different spatial scales. Model fit for each SDM specification was ranked from smallest AIC (i.e., rank = 1) to largest AIC (i.e., rank = 6) across all 100 backgrounds for each of the three buffers and for each species in scenario 1 and 2. The mean rank per SDM specification was then calculated for each species across each buffer in both scenarios and then the percentage of species associated to a given rank for each SDM specification was calculated. Rows represent scenarios, where panel (**A**) represents scenario 1 (all 301 amphibian species) and panel (**B**) represents scenario 2 (127 amphibian species having between 50 and 900 occurrences). Plot columns represent different spatial scales, where a given buffer size (i.e., 40%, 60%, and 80%, respectively) represents the radius (as a percentage of the maximum pairwise distances between a focal occurrence and each of its neighbours) within which background absences were sampled for species. Ranks are coloured and ordered by importance (i.e., high (lightest shade of blue = rank 1) to low (darkest shade of green = rank 6)). The SDM specifications are ordered and identified in the figure as follows: mean (i.e., model 1: between-patch climate heterogeneity), SD (i.e., model 2: within-patch climate heterogeneity), LSA (i.e., model 3: climate local spatial autocorrelation), Mean + SD (i.e., model 4: between-patch climate heterogeneity + within-patch climate heterogeneity), Mean + LSA (i.e., model 5: between-patch climate heterogeneity + climate local spatial autocorrelation), and Mean + SD + LSA (i.e., model 6: between-patch climate heterogeneity + within-patch climate heterogeneity + climate local spatial autocorrelation).

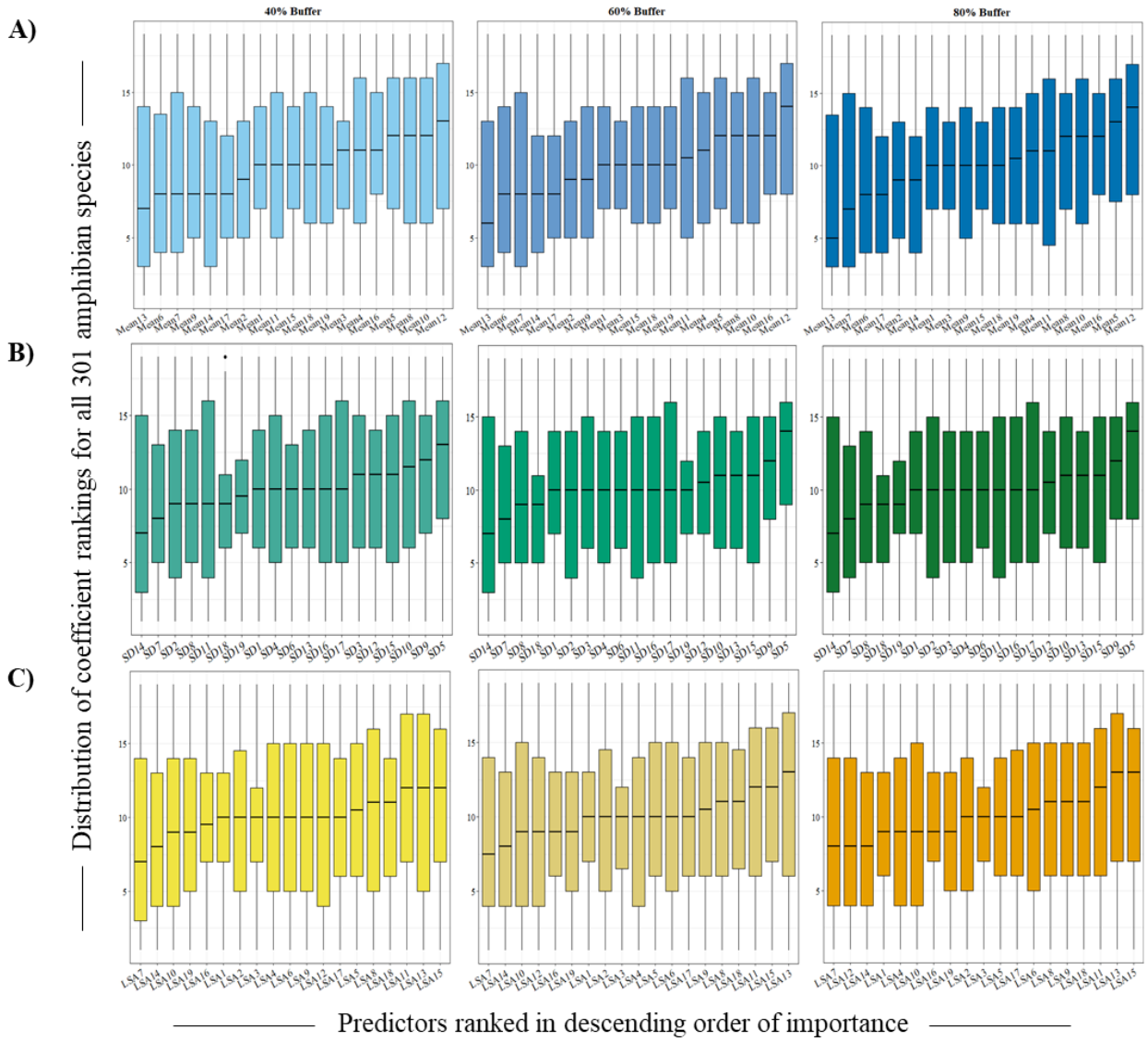

Figure 5: Within-model median coefficients rankings across all amphibian species for species distribution model (SDM) specifications of the Mean, SD, and SA of climate at different spatial scales. Coefficients for each of the 100-background data and three buffers for each of the 301 amphibian species were ranked within-model from largest (rank = 1) to smallest (rank = 19). This was done for (**A**) the Mean model (i.e., model 1 – between-patch climate heterogeneity) in blue, (**B**) the SD model (i.e., model 2- within-patch climate heterogeneity) in green, and (**C**) the LSA model (i.e., climate local spatial autocorrelation) in yellow. The median coefficient was taken over the 100-background data of each buffer, for each of the 19 model coefficients of each SDM specification across all species, giving a total of 301 median ranked coefficients per predictor and buffer, one for each species. Plot columns represent different spatial scales, where a given buffer size (i.e., 40% - lightest colour shade, 60% -medium colour shade, and 80% - darkest colour shade) represents the radius (as a percentage of the maximum pairwise distances between a focal occurrence and each of its neighbours) within which background absences were sampled for species. Rows represent the three (i.e., Mean, SD, and LSA) SDM specifications. Predictors (X-axis) of each SDM specification at each spatial scale, are ordered by importance, from most to least important.

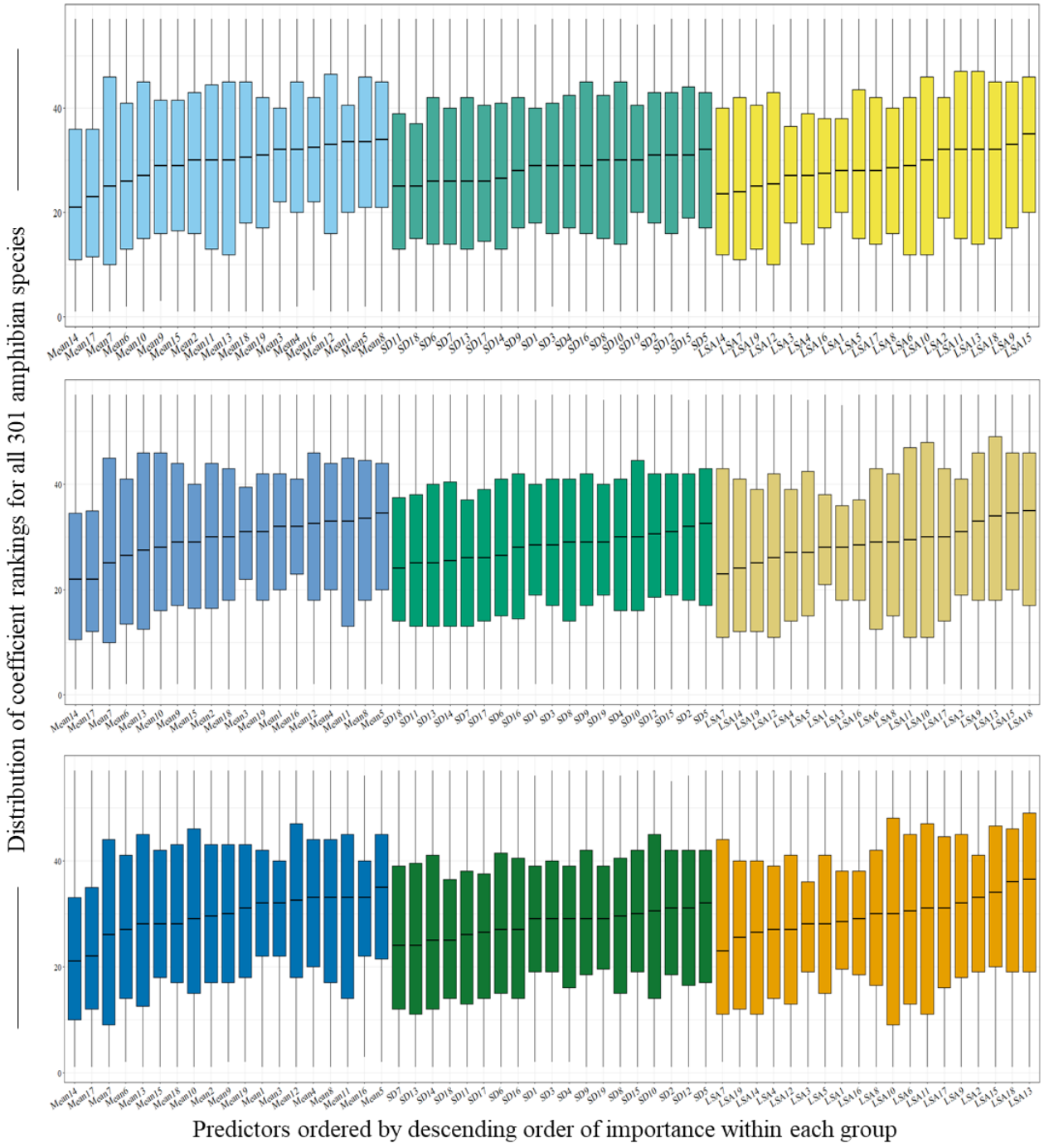

Figure 6: Within-model median coefficients rankings across all amphibian species for the species distribution model (SDM) specification with all climate predictors (i.e., Mean + SD + LSA) at different spatial scales. For this model (i.e., model 6 – between-patch climate heterogeneity + within-patch climate heterogeneity + climate local spatial autocorrelation), coefficients for each of the 100-background data and three buffers for each of the 301 amphibian species were ranked within-model from largest (rank = 1) to smallest (rank = 57). The median coefficient was then taken over the 100-background data of each buffer, for each of the 57 model coefficients of this model across all species, giving a total of 301 median ranked coefficients per predictor in each buffer, one for each species. Predictors (along the x-axis) at each spatial

scale are coloured according to type (i.e., Mean = blue, SD = green, LSA = yellow) and are ordered within-group by importance, from most to least important. Plot rows represent different spatial scales, where a given buffer size (i.e., 40% - lightest colour shade, 60% -medium colour shade, and 80% - darkest colour shade) represents the radius (as a percentage of the maximum pairwise distances between a focal occurrence and each of its neighbours) within which background absences were sampled for species.

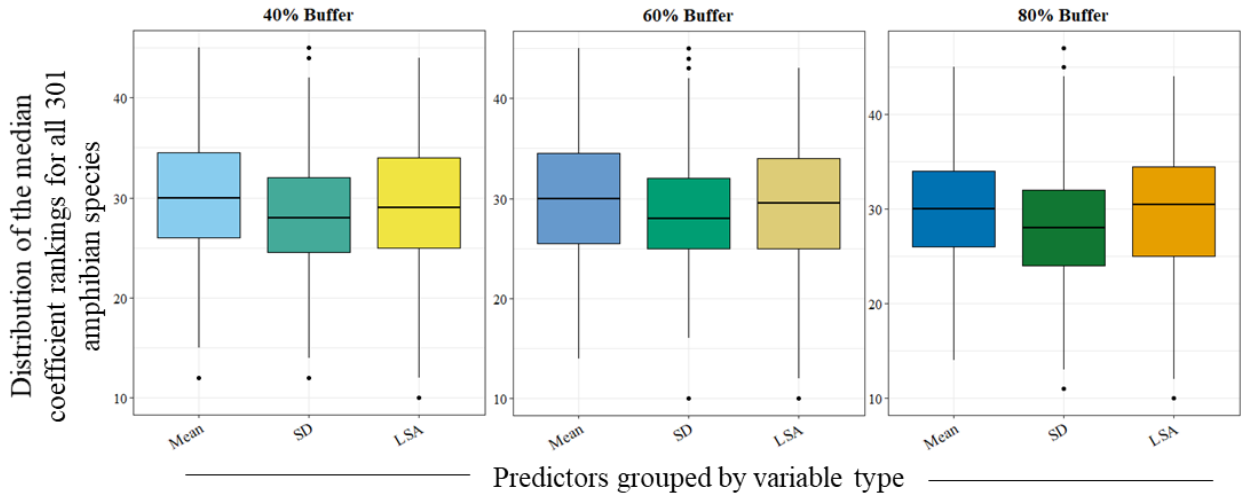

Figure 7: Group overall within-model median coefficients rankings across all amphibian species for each predictor type (i.e., Mean , SD, and LSA) of the species distribution model specification with all climate predictors at different spatial scales. For this model (i.e., model 6 – between-patch climate heterogeneity + within-patch climate heterogeneity + climate local spatial autocorrelation), coefficients of each predictor for each of the 100-background data and three buffers for each of the 301 amphibian species were ranked within-model from largest (rank = 1) to smallest (rank = 57). The coefficients were then grouped by predictor type (i.e., Mean, SD, or LSA) and the median (ranked coefficient) of each predictor (19 per type) was taken across all 100-background data for each species and each buffer, giving a total of 301 median ranked coefficients per predictor in each buffer, one for each species. Predictors (along the x-axis) at each spatial scale are coloured according to type (i.e., Mean= blue, SD = green, LSA = yellow). Plot columns represent different spatial scales, where a given buffer size (i.e., 40% - lightest colour shade, 60% -medium colour shade, and 80% - darkest colour shade) represents the radius (as a percentage of the maximum pairwise distances between a focal occurrence and each of its neighbours) within which background absences were sampled for species.

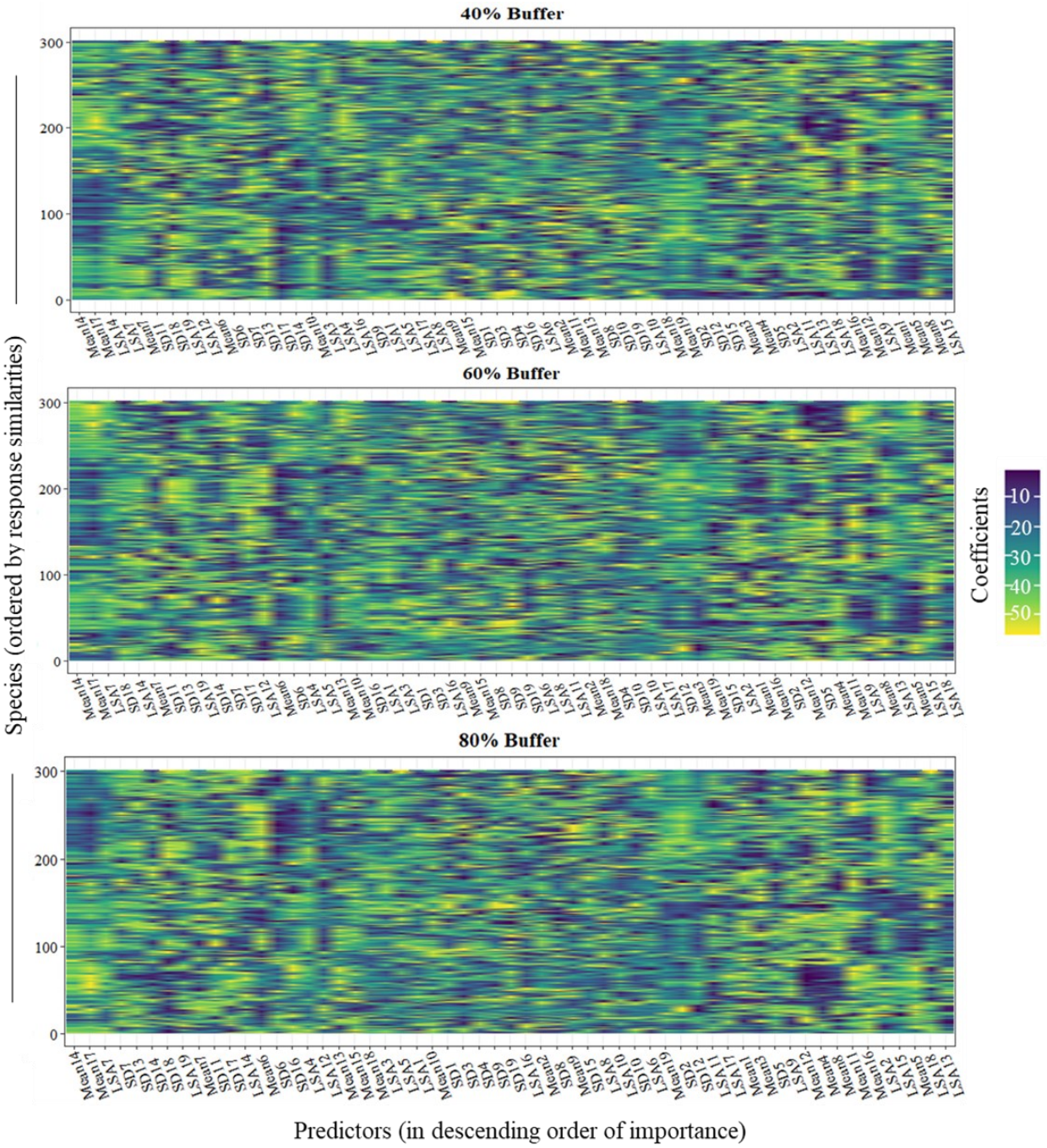

Figure 8: Heatmaps of amphibian species clustered by their response to within-model median coefficients rankings for the species distribution model (SDM) specification with all climate predictors (i.e., Mean + SD + LSA) at different spatial scales. For this model (i.e., model 6 – between-patch climate heterogeneity + within-patch climate heterogeneity + climate local spatial autocorrelation), coefficients for each of the 100-background data and three buffers for each of the 301 amphibian species were ranked within-model from largest (rank = 1) to smallest (rank = 57). The median of the ranked coefficients was then taken over the 100-background data of each buffer, for each of the 57 model predictors of this model across all species, giving a total of 301 (median ranked) coefficients (i.e., one for each of the 301 species) for each of the 57

predictors in each buffer. The heatmap is a result of a hierarchical cluster analysis performed to group species based on the similarities in their responses to the 57 predictors of this SDM specification. Predictors along the x-axis were then ranked by their median ranked coefficient values from smallest (rank = 1) to largest (rank = 57) ranked median coefficient and ordered from most important (highest rank) to least important (lowest rank). Coefficients (one for each of the 301 amphibian species), are colored based on their median ranked value within each predictor. Plot rows represent different spatial scales, where a given buffer size (i.e., 40%, 60%, and 80%) represents the radius (as a percentage of the maximum pairwise distances between a focal occurrence and each of its neighbours) within which background absences were sampled for species.

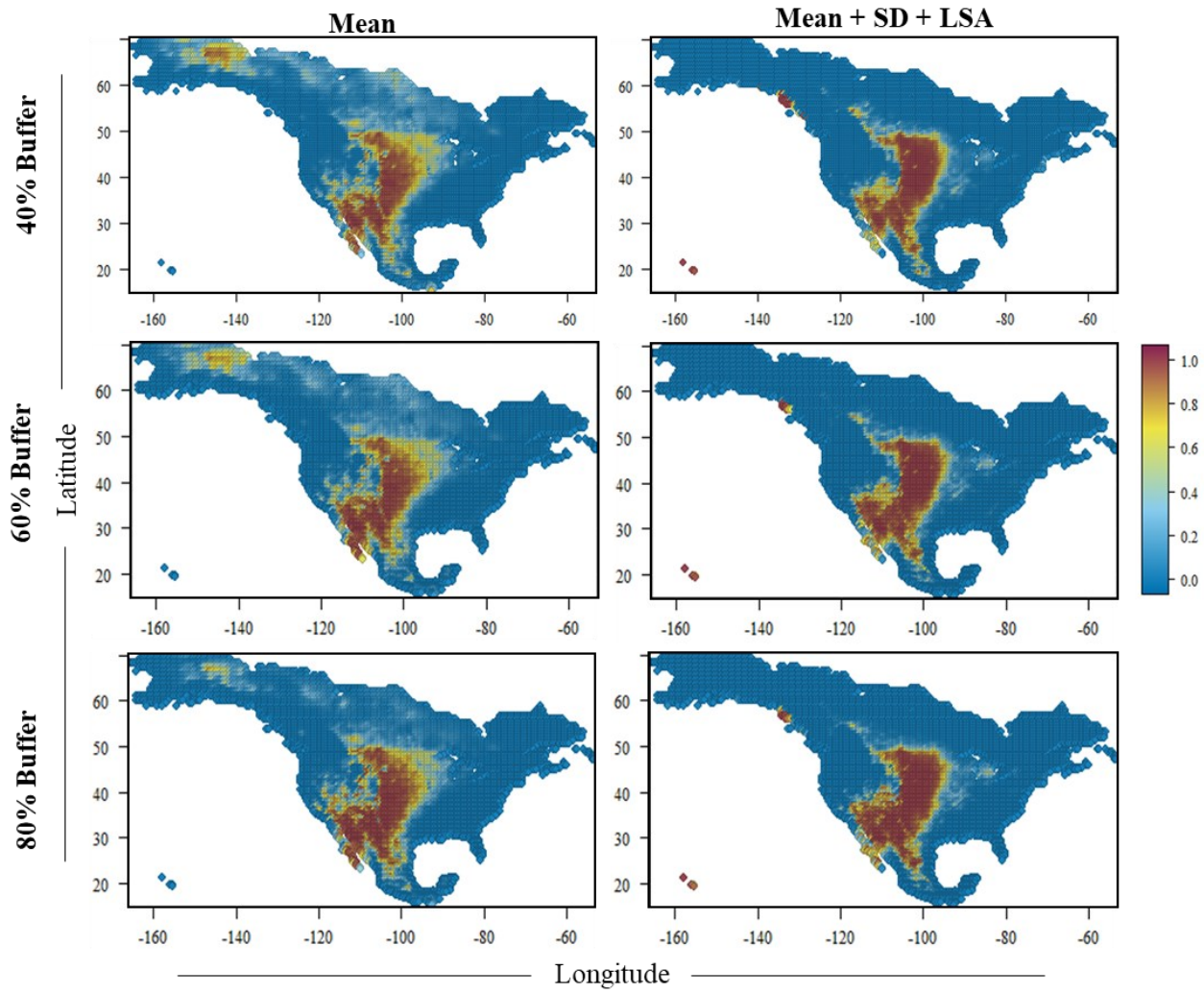

Figure 9: Predictions for the probability of presence in *Anaxyrus cognatus* (Great Plains toad) on continental North America and Hawaii for the predictive species distribution model (SDM) specifications for both the Mean and the all-predictor (i.e., Mean + SD + LSA) climate models at different spatial scales. Columns represent the two SDM specifications; Mean (i.e., between-patch climate heterogeneity; left), and Mean + SD + LSA (i.e., between-patch climate heterogeneity + within-patch climate heterogeneity + climate local spatial autocorrelation; right). Plot rows represent different spatial scales, where a given buffer size (i.e., 40%, 60%, and 80%) represents the radius (as a percentage of the maximum pairwise distances between a focal occurrence and each of its neighbours) within which background absences were sampled for species. The x and y-axes represent the longitude and latitude (respectively) coordinates of the geographic supercells (in decimal degrees (DD)) over which the predictions for the probability of presence have been made. The colour scalebar represents predicted absences (0 = blue) to presences (1 = red). Intermediate colours in the scalebar (light blue to orange = values > 0 and < 1) represent uncertainties in the predictions of presences and absences.

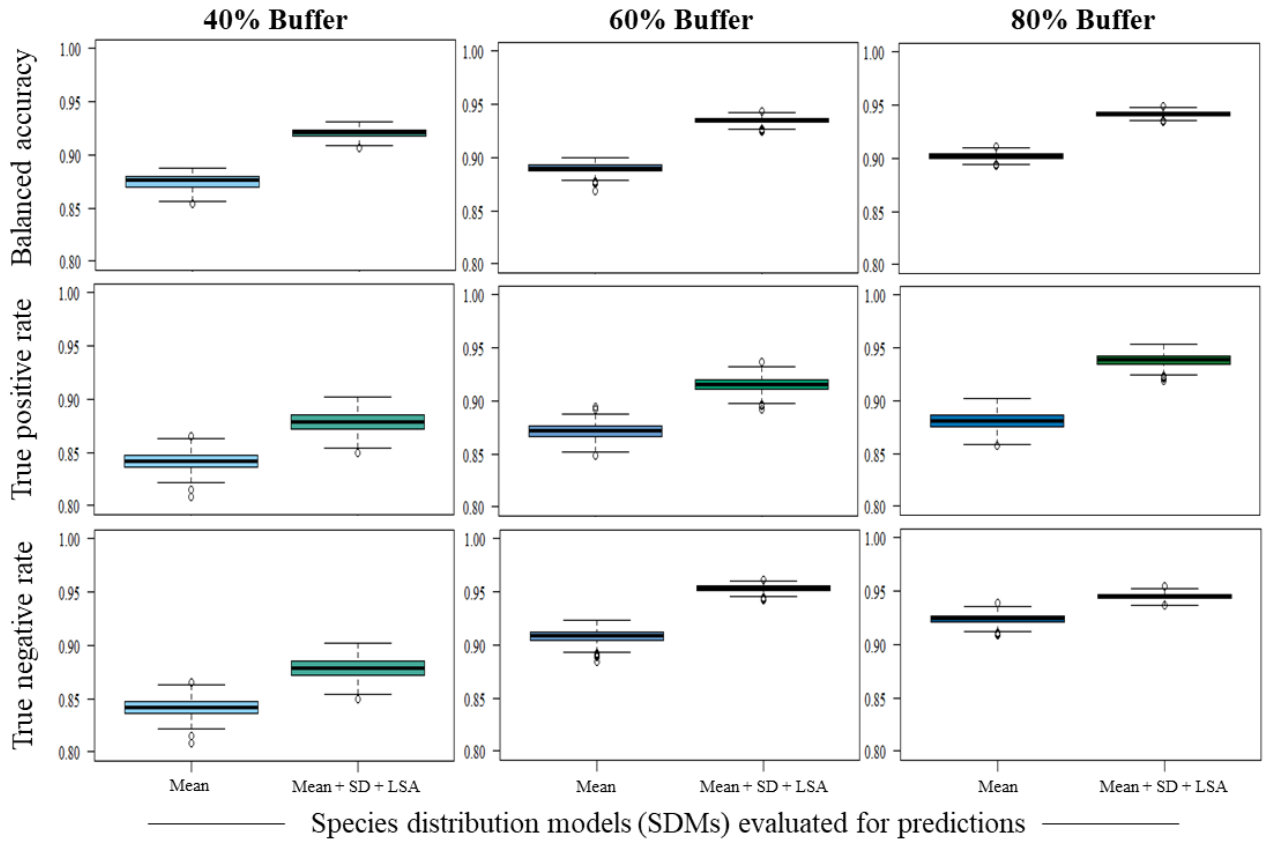

Figure 10: Measures of model performance for the predictive species distribution model (SDM) specifications for both the Mean and the all-predictor (i.e., Mean + SD + LSA) climate models at different spatial scales for *Anaxyrus cognatus* (Great Plains toad) on continental North America and Hawaii. Model performance was evaluated using three metrics: True Positive Rate (TPR) (i.e., number of cells where the species is predicted as present and is present), True Negative Rate (TNR) (i.e., the number of cells where the species is predicted as absent and is absent), and the balanced accuracy (i.e., (TPR + TNR)/2). Rows (y-axes) represent the metrics of model performance for each predictive SDM specification. The x-axis represents the predictive SDM specifications evaluated (i.e., Mean (blue) = between-patch climate heterogeneity, and mean + SD + LSA (green) = between-patch climate heterogeneity + within-patch climate heterogeneity + climate local spatial autocorrelation). Plot columns represent different spatial scales, where a given buffer size (i.e., 40% - lightest colour shade, 60% - medium colour shade, and 80% - darkest colour shade) represents the radius (as a percentage of the maximum pairwise distances between a focal occurrence and each of its neighbours) within which background absences were sampled for species.

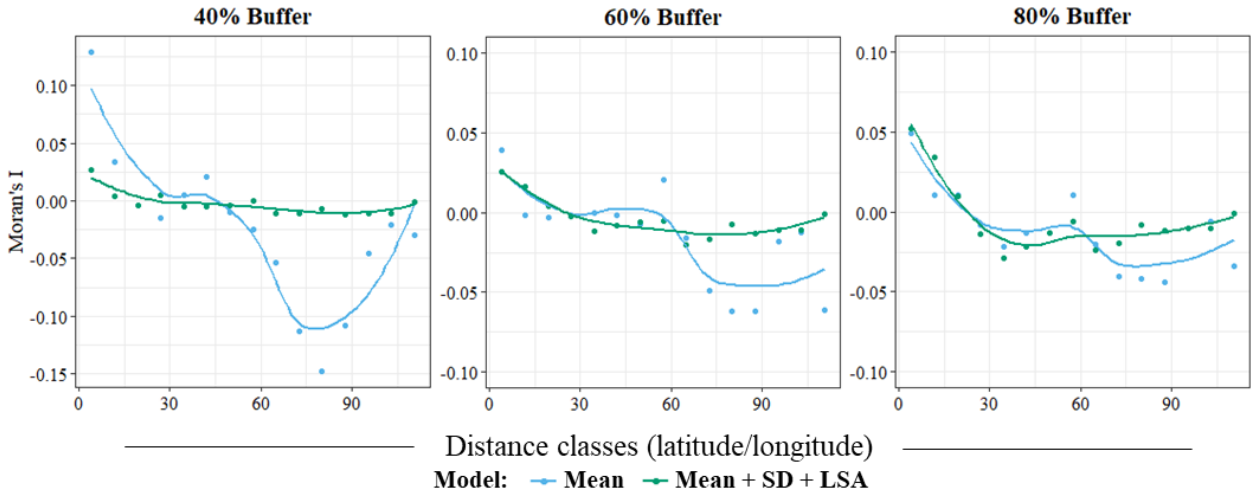

Figure 11: Comparison of the spatial autocorrelation of model residuals between both predictive species distribution model (SDM) specifications at different spatial scales for the case study species *Anaxyrus cognatus* (Great Plains toad). The predictive models tested were of the Mean (i.e., between-patch climate heterogeneity) climate variables (in blue) and the all-variable model (i.e., between-patch climate heterogeneity + within-patch climate heterogeneity + climate local spatial autocorrelation) (in green) for all 7035 geographic supercells representing all continental North American and Hawaii. Plot columns represent different spatial scales, where a given buffer size (i.e., 40%, 60%, and 80%) represents the radius (as a percentage of the maximum pairwise distances between a focal occurrence and each of its neighbours) within which background absences were sampled for species. Residual spatial autocorrelation here, is represented as a correlogram based on global Moran's *I*.

Table 1: Proportion (%) of amphibian species associated to the average ranking in model fit (i.e., AIC) for all six species distribution model specifications across three different spatial scales and for both scenarios 1 (all 301 amphibian species) and 2 (127 amphibian species having between 50 and 900 occurrences.

		40% Buffer						60% Buffer						80% Buffer					
		Rank 1	Rank 2	Rank 3	Rank 4	Rank 5	Rank 6	Rank 1	Rank 2	Rank 3	Rank 4	Rank 5	Rank 6	Rank 1	Rank 2	Rank 3	Rank 4	Rank 5	Rank 6
P = 301	Mean	16.61	32.89	24.58	5.98	19.93	0.00	19.27	32.89	24.25	5.98	17.28	0.00	18.94	38.21	21.59	6.31	14.62	0.00
	SD	25.58	5.65	20.60	2.99	6.64	38.21	23.26	6.31	23.26	3.32	6.31	37.54	21.93	7.31	24.58	1.99	6.31	37.87
	LSA	30.56	29.90	16.94	14.29	7.97	0.00	33.89	32.56	13.95	12.96	6.31	0.00	38.54	29.90	14.29	10.30	6.64	0.00
	Mean + SD	4.98	5.98	30.23	55.15	3.32	0.00	3.99	6.64	26.91	56.81	5.65	0.00	2.66	5.98	29.24	57.48	4.32	0.00
	Mean + LSA	7.97	16.94	5.32	17.61	50.50	1.33	9.63	14.29	7.31	15.61	52.82	0.33	10.30	11.63	7.31	17.61	53.16	0.00
	Mean + SD + LSA	14.00	8.00	2.00	4.00	11.00	60.00	10.00	7.00	4.00	5.00	12.00	62.00	8.00	7.00	2.00	6.00	15.00	62.00
$50 \leq P \leq 900$	Mean	18.11	24.41	14.17	9.45	33.86	0.00	19.69	32.28	9.45	9.45	29.13	0.00	21.26	37.01	7.09	8.66	25.98	0.00
	SD	0.79	1.57	7.09	4.72	11.81	74.02	1.57	0.79	10.24	3.94	10.24	73.23	0.79	1.57	11.02	3.15	9.45	74.02
	LSA	33.07	18.11	13.39	21.26	14.17	0.00	38.58	18.90	12.60	19.69	10.24	0.00	44.88	20.47	10.24	16.54	7.87	0.00
	Mean + SD	11.02	11.81	48.03	26.77	1.57	0.00	9.45	12.60	42.52	27.56	7.87	0.00	6.30	12.60	48.82	25.98	5.51	0.00
	Mean + LSA	18.90	24.41	12.60	28.35	14.17	0.79	19.69	22.05	15.75	26.77	14.96	0.79	20.47	16.54	16.54	30.71	15.75	0.00
	Mean + SD + LSA	18.00	20.00	5.00	9.00	24.00	25.00	11.00	13.00	9.00	13.00	28.00	26.00	6.00	12.00	6.00	14.00	35.00	26.00

Note:

Ranks are in decreasing order of importance, where Rank 1 is the highest rank and Rank 6 is the lowest. Ranks are attributed to AIC values; where the lowest AIC value (best fitted model) is assigned a rank of 1 and the highest AIC value (worst fitted model) is assigned a rank of 6.

[1] P = 301 designates the presences for all 301 amphibian species

[2] $50 \leq P \leq 900$ designates amphibian species having between 50 and 900 presences (127 species)

[3] Mean (model 1) = between-patch climate heterogeneity; SD (model 2) = within-patch climate heterogeneity; LSA (model 3) = climate local spatial autocorrelation; Mean + SD (model 4) = between-patch climate heterogeneity + within-patch climate heterogeneity, Mean + LSA (model 5) = between-patch climate heterogeneity + climate local spatial autocorrelation; Mean + SD + LSA (model 6) = between-patch climate heterogeneity + within-patch climate heterogeneity + climate local spatial autocorrelation

[4] The 40%, 60%, and 80% buffers, respectively, are the three spatial scales representing the radius (as a percentage of the maximum pairwise distances between a focal occurrence and each of its neighbours) within which background absences were sampled for species

APPENDIX I

The 19 bioclimatic variables from WorldClim (Fick and Hijmans 2017) used in this thesis are listed as the following:

BIO1 = Annual Mean Temperature

BIO2 = Mean Diurnal Range (Mean of monthly (max temp – min temp))

BIO3 = Isothermality (BIO2/BIO7)*100

BIO4 = Temperature Seasonality (standard deviation*100)

BIO5 = Max Temperature of Warmest Month

BIO6 = Min Temperature of Coldest Month

BIO7 = Temperature Annual Range (BIO5-BIO6)

BIO8 = Mean Temperature of Wettest Quarter

BIO9 = Mean Temperature of Driest Quarter

BIO10 = Mean Temperature of Warmest Quarter

BIO11 = Mean Temperature of Coldest Quarter

BIO12 = Annual Precipitation

BIO13 = Precipitation of Wettest Month

BIO14 = Precipitation of Driest Month

BIO15 = Precipitation Seasonality (Coefficient of Variation)

BIO16 = Precipitation of Wettest Quarter

BIO17 = Precipitation of Driest Quarter

BIO18 = Precipitation of Warmest Quarter

BIO19 = Precipitation of Coldest Quarter

When referencing the *Mean* ($\bar{X}$), *SD* (***s***), and *LSA* of the bioclim variables throughout the text, they designate the mean (i.e., between-patch climate heterogeneity), standard deviation (within-patch climate heterogeneity), and spatial autocorrelation (climate local spatial autocorrelation) of each of the 19 bioclim variables listed above.

Table A1: Overall average and median rankings of model fit (based on AIC) for the six species distribution model specifications evaluated across three different spatial scales and for both scenarios 1 (all 301 amphibian species) and 2 (127 amphibian species having between 50 and 900 presences).

	40% Buffer				60% Buffer				80% Buffer			
	Overall Mean		Overall Median		Overall Mean		Overall Median		Overall Mean		Overall Median	
	Rankings											
	P = 301	50 ≤ P ≤ 900	P = 301	50 ≤ P ≤ 900	P = 301	50 ≤ P ≤ 900	P = 301	50 ≤ P ≤ 900	P = 301	50 ≤ P ≤ 900	P = 301	50 ≤ P ≤ 900
Mean	2	4	2	4	2	2	2	2	2	2	2	2
SD	4	6	3	6	4	6	3	6	4	6	3	6
LSA	1	1	1	1	1	1	1	1	1	1	1	1
Mean + SD	3	3	4	3	3	4	4	4	3	4	4	3
Mean + LSA	5	2	5	2	5	2	5	3	5	3	5	4
Mean + SD + LSA	6	5	6	5	6	5	6	5	6	5	6	5

Note:

Ranks are in descending order of importance, where 1 is the most important and 6 is the least important

[1] P = 301 designates all presences (301 amphibians species);

[2] 50 ≤ P ≤ 900 designates species having between 50 and 900 presences (127 amphibians species)

[3] Mean (model 1) = between-patch climate heterogeneity; SD (model 2) = within-patch climate heterogeneity; LSA (model 3) = climate local spatial autocorrelation; Mean + SD (model 4) = between-patch climate heterogeneity + within-patch climate heterogeneity, Mean + LSA (model 5) = between-patch climate heterogeneity + climate local spatial autocorrelation; Mean + SD + LSA (model 6) = between-patch climate heterogeneity + within-patch climate heterogeneity + climate local spatial autocorrelation

[4] The 40%, 60%, and 80% buffers, respectively, are the three spatial scales representing the radius (as a percentage of the maximum pairwise distances between a focal occurrence and each of its neighbours) within which background absences were sampled for species